Chapter 6
Performance Evaluation of Integrated Energy Systems

Pouria Ahmadi, Ibrahim Dincer and Marc A. Rosen

Abstract The current literature on integrated energy systems for various applications is discussed and how energy systems are integrated for multigeneration purposes is explained. Three integrated energy systems, including renewable and non-renewable ones, are considered to enhance the analyses. A micro-gas turbine integrated system is selected as the non-renewable system while biomass and ocean thermal energy conversion based energy systems are considered as the renewable options. Exergy analysis is conducted to determine the irreversibilities in each component and the system performance. Furthermore, economic and environmental impact assessments of the systems are conducted, and the results are presented for each integrated system. The results show that the integrated energy systems have higher exergy efficiency compared to single generation unit and that the integration results in reduction of greenhouse gases emission. The performances of the three systems are compared, and the results show that the choice and benefits of integrated systems strongly depends on the priorities of the designers and engineers.

Keywords Energy · Exergy · Efficiency · Integrated energy system

6.1 Introduction

Energy use is directly linked to well-being and prosperity across the world. Meeting the growing demand for energy in a safe and environmentally responsible manner is an important challenge. A key driver of energy demand is the human desire to sustain and improve ourselves, our families and our communities. There are around 7 billion people on Earth and population growth will likely lead to an increase in energy demand, which depends on the adequacy of energy resources. Increasing population

I. Dincer (✉)
Department of Mechanical Engineering, University of Ontario Institute of Technology (UOIT), 2000 Simcoe St. North, Oshawa, ON L1H 7K4, Canada
e-mail: ibrahim.dincer@uoit.ca

P. Ahmadi · M. A. Rosen
Faculty of Engineering and Applied Science, University of Ontario Institute of Technology (UOIT), 2000 Simcoe St. North, Oshawa, ON L1H 7K4, Canada

I. Dincer et al. (eds.), *Progress in Sustainable Energy Technologies: Generating Renewable Energy,* DOI 10.1007/978-3-319-07896-0_6,

and economic development in many countries are having serious implications for the environment, because energy generation processes (e.g., generation of electricity, heating, cooling, and shaft work for transportation and other applications) emit pollutants, many of which are harmful to ecosystems. Burning fossil fuels results in the release of large amounts of greenhouse gases, particularly carbon dioxide.

Energy exists in several forms, e.g. light, heat, and electricity. Concerns exist regarding limitations to easily accessible supplies of energy resources and the contribution of energy processes to global warming as well as other environmental concerns such as air pollution, acid precipitation, ozone depletion, forest destruction, and radioactive emissions [1]. There are various alternative energy options to fossil fuels, including solar, geothermal, hydropower, wind and nuclear energy. The use of many of the available natural energy resources is limited due to their reliability, quality and energy density. Nuclear energy has the potential to contribute a significant share of large scale energy supply without contributing to climate change. Advanced technologies, aimed at mitigating global warming, are being proposed and tested in many countries. Among these technologies, multigeneration processes, including trigeneration, can make important contributions due to their potential for high efficiencies as well as low operating costs and pollution emissions per energy output. Issues like fossil fuel depletion and climate change amplify the advantages and significance of efficient multigeneration energy systems.

Global warming, which is one the facets of global climate change, refers to an increase in the average temperature of the atmosphere and oceans, which appears to have occurred in recent decades and is projected to continue. The drivers of climate change are generally agreed to be changes in the atmospheric concentrations of greenhouse gases (GHGs) and aerosols. According to the Intergovernmental Panel on Climate Change (IPCC), most of the increase in global average temperatures since the mid-twentieth century is linked to the observed increase in anthropogenic GHG concentrations. A greenhouse gas is a gas in an atmosphere that absorbs and emits radiation within the thermal infrared range [2]. This process is the fundamental cause of the greenhouse effect.

The primary greenhouse gases in the Earth's atmosphere are water vapor, carbon dioxide, methane, nitrous oxide, and ozone. The greenhouse effect is a process by which thermal radiation from a planetary surface is absorbed by atmospheric greenhouse gases, and is re-radiated in all directions. Since part of this re-radiation is back towards the surface and the lower atmosphere, it results in an elevation of the average surface temperature above what it would be in the absence of the gases [2]. Global warming is agreed by many to be a direct effect of GHG emissions, which have increased notably over the last century.

Human activity since the Industrial Revolution has increased the amount of greenhouse gases in the atmosphere, leading to increased radioactive forcing from CO_2, methane, tropospheric ozone, chlorofluorocarbons (CFCs) and nitrous oxide. The effect of greenhouse gases on global warming is assessed using an index called global warming potential (GWP), which is a measure of how much a given mass of GHG contributes to global warming relative to a reference gas (usually CO_2) for which the GWP is set to 1. For a 100-year time horizon, GWPs of CO_2, CH_4 and

N_2O are reported to be 1, 25 and 298, respectively [3]. Using this index, one can calculate the equivalent CO_2 emissions by multiplying the emission of a GHG by its GWP. The main causes of global warming are as follows [3]:

- Carbon dioxide emissions from fossil fuel burning power plants.
- Carbon dioxide emissions from burning gasoline for transportation.
- Methane emissions from animals, agriculture such as rice paddies, and from Arctic sea beds.
- Deforestation, especially tropical forests for wood, pulp, and farmland.
- Use of chemical fertilizers on croplands.

CO_2 is widely believed to be a significant cause of global warming. The literature shows that concentrations of CO_2 and methane have increased by 36 and 148 % respectively since 1750 [3]. Fossil fuel combustion is responsible for about three-quarters of the increase in CO_2 from human activity over the past 20 years. The rest of this increase is caused mostly by changes in land use, particularly deforestation. The main source of CO2 emissions is fossil fuel-based electricity generation units, which account for about 32 % of the total CO2 emissions. The next largest source of CO2 emissions are caused by heating and cooling, which account for about 33 % of total CO_2 emissions, followed by emissions from cars and trucks, which account for 23 % of total global CO_2 emissions, and other major transportation, which accounts for 12 % [3]. Hence, about 65 % of the total CO_2 emissions are attributable to electricity generation and heating and cooling, both of which are directly associated with energy needs of human beings.

Cogeneration, or combined heat and power (CHP), represents a relatively simple, integrated multigeneration energy system involving the use of waste or other heat from electricity generation to produce heating. The overall energy efficiency of a cogeneration system, defined as the part of the fuel converted to both electricity and useful thermal energy, is typically 40–50 % [4] but can be much higher. Recently, researchers have extended CHP to trigeneration, a system for the simultaneous production of heating, cooling and electricity from a common energy source. Trigeneration often utilizes the waste heat of a power plant to improve overall thermal performance [5], and is suitable for some energy markets.

The benefits of integrating energy systems became prominent with the application of cogeneration for heat and electricity production. In this simple energy system, waste or other heat is used to produce either cooling or heating. In general, cogeneration is the production of heat and electricity in one process using a single energy source, which often yields considerable reductions in input energy compared to separate processes. Cogeneration is often associated with the combustion of fossil fuels, but can also be carried out using certain renewable energy sources, nuclear energy, and waste thermal energy (obtained directly or by burning waste materials). The recent trend has been to use cleaner fuels for cogeneration, such as natural gas. The strong long-term prospects for cogeneration in global energy markets are related to its ability to provide significant operational, environmental and financial benefits. The product thermal energy from cogeneration can be used for domestic hot water heating, space heating, pool heating, laundry heating processes

and absorption cooling. The more the product heat from cogeneration can be used in existing systems, the more financially attractive the system is. Cogeneration helps overcome a drawback of many conventional electrical and thermal systems: significant heat losses, which detract greatly from efficiency [5]. Heat losses are reduced and efficiency is increased when cogeneration is used to supply heat to various applications and facilities.

The overall energy efficiency of a cogeneration system is the percent of the fuel converted into both electricity and useful thermal energy. Recently, researchers have extended CHP to have more output purposes. In this regard, trigeneration energy systems have become more suitable for energy markets. Trigeneration is the simultaneous production of heating, cooling and electricity from a common energy source. Trigeneration utilizes the waste or other heat of a power plant to improve overall thermal performance, often utilizing the free energy available from waste energy. In a trigeneration system, waste heat from the plant's prime mover (e.g, gas turbine or diesel engine or Rankine cycle [6]), sometimes with temperature enhancement, drives heating and cooling devices. The heat can be used for space heating, domestic hot water production or steam production for process heating. The heat can also be used for cooling, by driving an absorption chiller. Several studies on trigeneration have been conducted in the last few years, likely due to its benefits and plans for applications. Trigeneration can be applied widely, e.g., in chemical and food industries, airports, shopping centres, hotels, hospitals, and houses. Figure 1.1 illustrates a trigeneration energy system, consisting of the following three major parts:

- A power generation unit, i.e. a prime mover, such as a gas turbine.
- A cooling unit, such as a single-effect absorption chiller.
- A heating unit, such as a boiler or heat recovery steam generator.

The following processes occur in a trigeneration plant:

- Mechanical power is produced via a generator unit, such as a gas turbine.
- The mechanical power is used to drive an electrical generator.
- Waste heat exits the mechanical generator unit directly or via heated materials like exhaust gases.

As shown in Fig. 6.1, with a single prime mover we can produce heating, cooling and electricity simultaneously. Recently, researchers have extended trigeneration to produce more products like hot water, hydrogen and potable water using a single prime mover via multigeneration.

The efficiencies for multigeneration energy systems can be higher than those for either trigeneration or CHP because of the additional products (hydrogen, potable and hot water, etc.). Figures 6.2 and 6.3 illustrate two multigeneration energy systems. The system in Fig. 6.2 produces electricity, cooling, heating, hot water and hydrogen. To produce hydrogen, an electrolyzer is used, which is driven by part of the electricity generated by a solar concentrating collector. Hot water enters the electrolyzer and is reacted electrochemically to split its molecules into hydrogen and oxygen. The heating system is composed of two parts, one for hot water

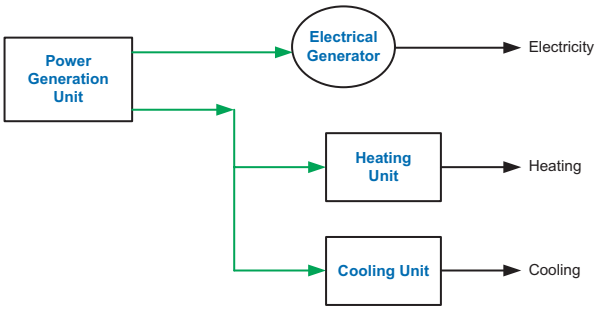

Fig. 6.1 A typical trigeneration energy system [5]

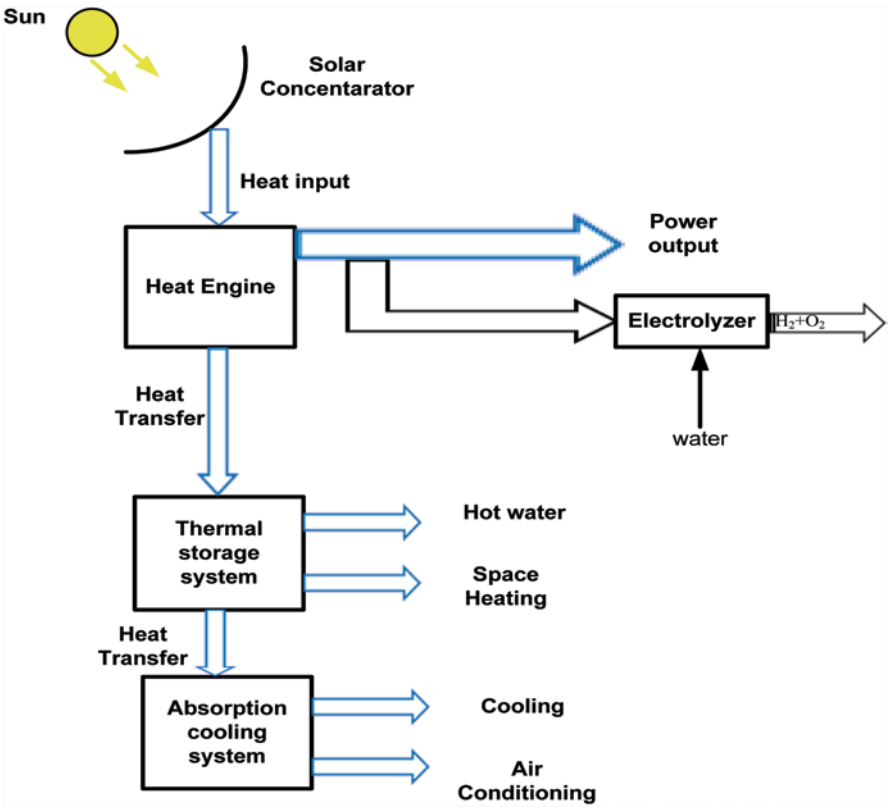

Fig. 6.2 A multigeneration energy system for producing electricity, cooling, heating, hot water and hydrogen [7]

production and another for space heating. Heat rejected from the storage system enters the absorption cooling system to produce cooling and air conditioning. If the system is extended to produce potable water, a desalination system must be used, and such a multigeneration energy system is shown in Fig. 6.3. In this case, a portion of the heat produced by the solar concentrator is used to run a desalination

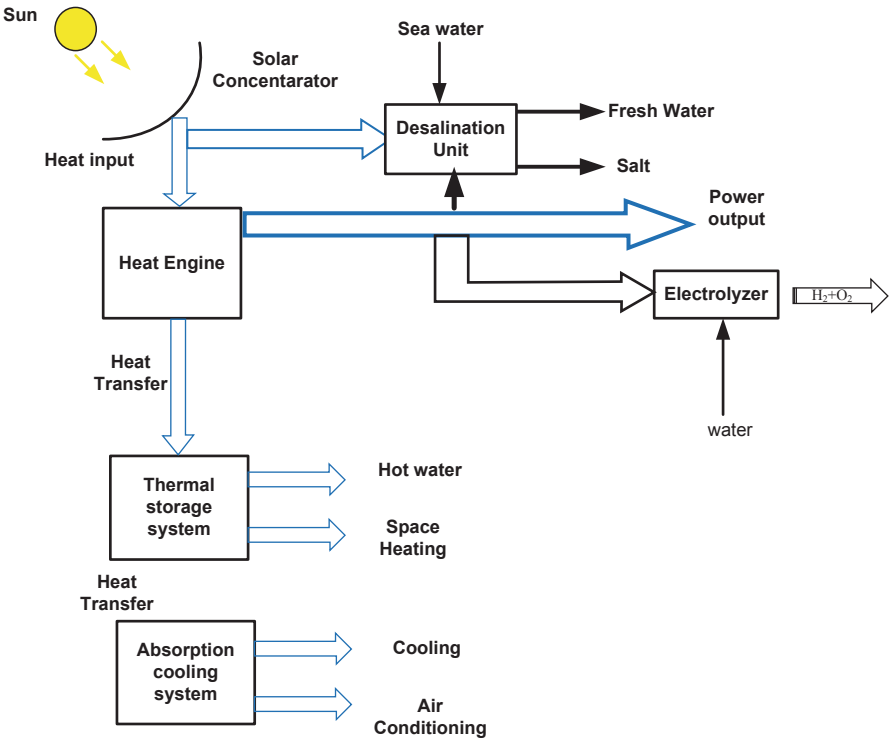

Fig. 6.3 A multigeneration energy system for producing electricity, cooling, heating, hot water, hydrogen and fresh water [7]

system, while part of the electricity generated by the power unit drives the pumps. Other parts of the system are the same as in Fig. 6.2. These two figures are representative of typical multigeneration energy systems that use only solar energy as an input. Other configurations that combine renewable and conventional energy sources are also possible, and are discussed subsequently.

Benefits of Integrated Energy Systems

There are many benefits of integrated energy systems, including higher plant efficiency, reduced thermodynamic losses and wastes, reduced operating costs, reduced greenhouse gas emissions, better use of resources, shorter transmission lines, fewer distribution units, multiple generation options, increased reliability, and less grid failure [7]. These benefits are discussed below. Integrated systems improve the overall efficiency of the plant and reduce the operating costs. The overall efficiency of conventional power plants that use fossil fuel with a single prime mover is usually less than 40%. That is, more than 60% of the heating value of the fuel energy entering a conventional power plant is lost. On the other hand, the overall efficiency of a conventional power plant that produces electricity and heat separately is around 60% or more [8].

However, with the utilization of the waste heat from the prime mover, the efficiency of multigeneration plants could reach up to 80% [9]. In a multigeneration plant, the waste heat from the electricity generation unit is used to operate the cooling and heating systems without the need for extra fuel, unlike a conventional power plant that requires extra energy resources. Thus, a multigeneration plant uses less energy to produce the same output as a conventional plant, and has correspondingly lower operating costs.

Integrated systems also reduce GHG emissions. Since a multigeneration energy system uses less fuel to produce the same output compared to a conventional power plant, a multigeneration plant emits less GHGs. Although the GHG emissions from multigeneration plants are less than conventional plants, there are some limitations of using multigeneration plants in a distributed manner because of their on-site gas emissions. Another important benefit of using multigeneration energy systems is that they reduce costs and energy losses due to the fact that they need fewer electricity transmission lines and distribution units. The conventional production of electricity is usually from a centralized plant that is generally located far from the end user. The losses from transmission and distribution of electricity from a centralized system to the user can be about 9% [8].

These benefits have encouraged researchers and designers to develop multigeneration energy systems. The improvement in efficiency is often an important factor in implementing a multigeneration energy system. Further assessments before selecting multigeneration plants, such as evaluations of initial capital and operating costs, are needed to ensure efficient and economic multigeneration plant construction and performance [8].

Multigeneration Energy Systems

A multigeneration energy system usually refers to a system with more than three different purposes from the same source of input energy (the prime mover). These purposes can include electricity, cooling, heating, hot water, hydrogen and fresh water. These systems should be considered for residential application, power plants and other places where numerous useful outputs are required. It must be noted that the location and requirements of its application are major factors the design of a multigeneration energy system. For example, in a place where the need for fresh water is vital, a multigeneration system meant to address the need must prioritize this purpose. In the literature, there are few studies on focused on optimizing multigeneration energy systems. These systems are have the potential to help address global warming.

It is worth mentioning that different methods are available to achieve each purpose of multigeneration energy systems; this is why the application of each subsystem is very important in meeting the system's requirements. Figure 6.6 shows a practical multigeneration energy system to produce electricity, cooling, power and domestic hot water that works based on a gas turbine Brayton cycle. In order to produce saturated steam in this multigeneration system, a dual pressure heat

recovery steam generator (HRSG) is used. High pressure saturated steam enters a steam turbine to produce electricity while lower pressure steam works as an absorption chiller heat input into the generator. In order to produce the cooling demand, a single effect absorption chiller with Li-Br water as working fluid is employed. Saturated liquid leaves the generator, which is then used to heat up water using a domestic water heater. According to the concept of a Rankine cycle, the condenser rejects an amount of heat. This heat could be considered either for the space heating application or for a thermochemical water splitting cycle to produce hydrogen. As illustrated in Fig. 6.4, where the fuel is just injected into the combustion chamber, it is observed that this system has less environmental impact compared to GT cycles, CHP systems and trigeneration energy systems. The reason is due to this fact that waste heat from GT and CHP systems is used to produce cooling and heating applications. Energy efficiency of this cycle can exceed 70 %. This multigeneration system could be used to produce hydrogen, another valuable purpose. In this case, a part of the produced electricity could be used to drive an electrolyzer to produce hydrogen, which could then be used for either hybrid electric vehicles or to produce electricity using a fuel cell. As shown in Fig. 6.5, flue gases leave the HRSG at a temperature around 150 °C. To increase the efficiency of this multigeneration system, the energy of these flue gases could be utilized in a heat exchanger and produce more electricity and cooling by using an ejector refrigeration system. With this configuration, the efficiency of the system could be higher than 85 %.

Figure 6.5 shows another multigeneration energy system for production of electricity, heating, cooling and fresh water. A photovoltaic solar panel is selected to use solar energy in order to run triple effect absorption to provide cooling. A triple effect absorption cooling system is also considered for the cooling demand of the system, and a desalination unit is applied to produce fresh water. In addition, Figs. 6.4 and 6.5 demonstrate the significant potential of multigeneration energy systems. There are many more options in the design multigeneration energy systems, which are discussed in detail in the following sections.

6.2 Review of Recent Advances

Various studies associated with CHP and trigeneration energy systems have been reported in the literature, although comprehensive studies of multigeneration energy systems are rare. Because of the environmental concerns and technological developments in the last decade, both the need and the capability of producing multipurpose energy solutions have been amplified considerably. The related papers, their aims, method of analysis and brief conclusions are presented in this section. We have tried to focus on the most recent studies regarding combined heat and power (CHP), trigeneration and multigeneration energy systems. Since there are several papers about CHP and trigeneration systems, the literature has been categorized based on thermodynamic modeling, exergy, exergoeconomic and exregoenvironmental analyses and optimization.

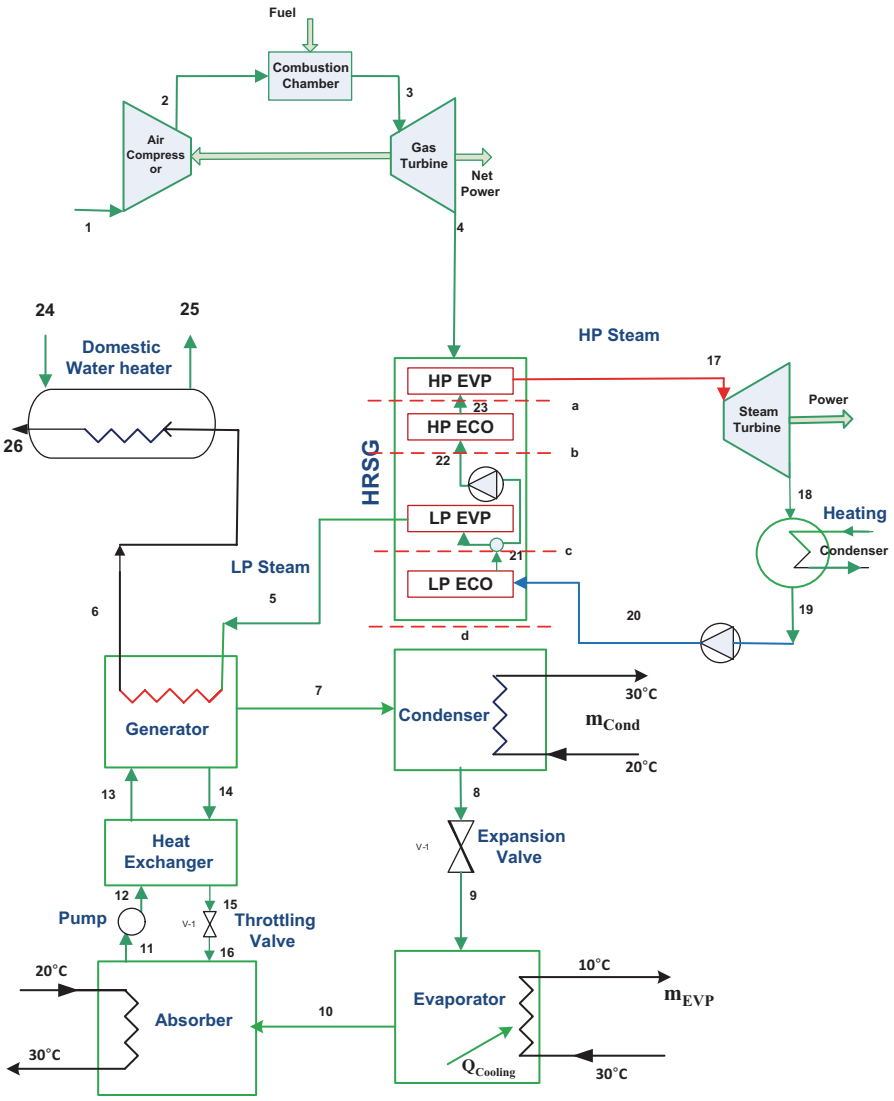

Fig. 6.4 Schematic of a multigeneration system for electricity, heating, cooling and hot water [5]

Cogeneration Heat and Power (CHP) Systems

An integrated energy system produces several useful outputs from one or more kinds of energy inputs. The main purposes of energy integration are usually to increase efficiency and sustainability of the system and to reduce environmental impact and cost of the system. Such systems often provide significant potential for

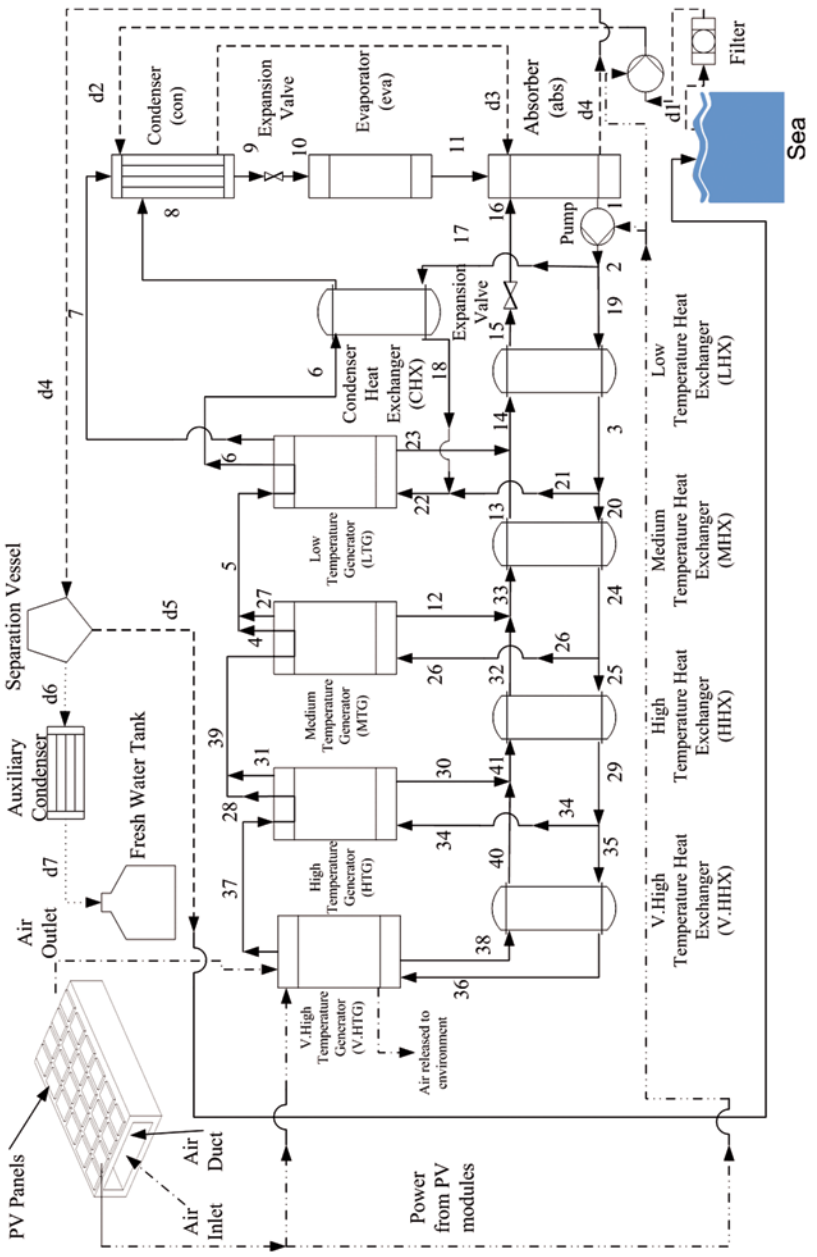

Fig. 6.5 Schematic diagram of a multigeneration energy system including desalination [10]

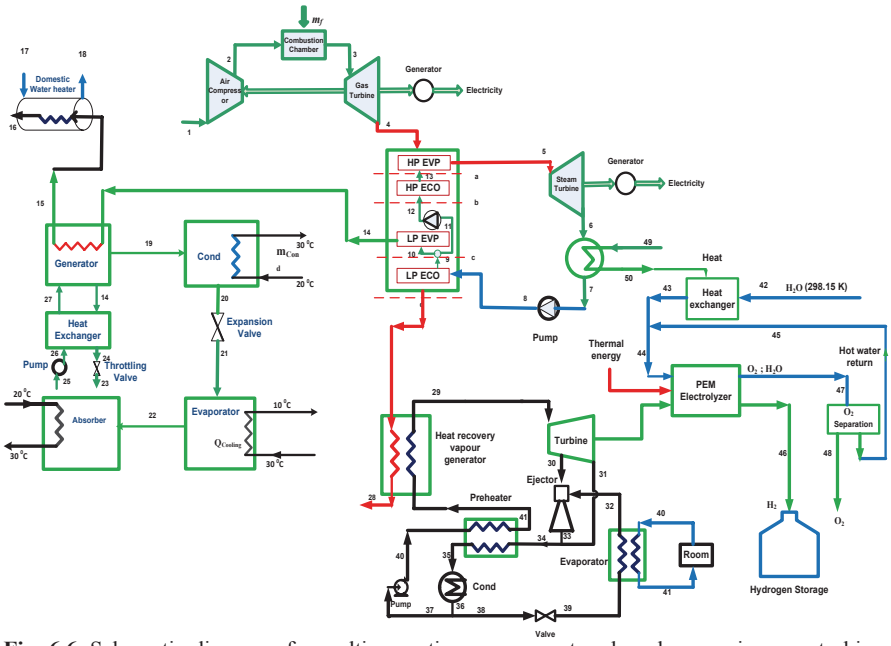

Fig. 6.6 Schematic diagram of a multigeneration energy system based on a micro gas turbine, a dual pressure heat recovery steam generator, an absorption chiller, and an ejector refrigeration cycle [5]

global warming mitigation. Multigeneration energy system as a potential example of integrated system can possibly produce some useful outputs including electricity, heating, cooling, hot water, fresh water and hydrogen. Cogeneration, or CHP, represents a relatively simple process that produces two commodities in an integrated fashion, including the use of waste heat from electricity generation to produce heating. The overall energy efficiency of a cogeneration system, defined as the part of the fuel energy content converted to both electricity and useful thermal energy, is typically 40–50 % and, in some cases, higher [11, 12, 13].

A micro-scale building cooling, heating and power (BCHP) system with an adsorption chiller was experimentally studied by Huangfu et al. [14]. The authors observed the performance of an adsorption chiller under different heating conditions. They concluded that there was an almost linear relation between the adsorption chiller and the change in hot water inlet temperature for the two investigated models. Mago et al. [15] analyzed and optimized the use of CHP-ORC systems for small commercial buildings. In another study, Mago et al. [16] reported on the evaluation of the potential emission reductions from the use of CHP systems in different commercial buildings. Mago and Hueffed [17] evaluated a turbine-driven combined cooling, heating and power (CCHP) system for large office buildings under various operating strategies, and explored the use of carbon credits to show how the possible reduction in carbon dioxide emissions via a CCHP system could translate into economic benefits.

Bianchi et al. [18] studied the performance analysis of an integrated CHP system with thermal and electric energy storage for residential application. Athanasovici et al. [4] proposed a unified comparison method for the thermodynamic efficiency of CHP plants, and used this method to compare various separate and combined energy production processes. Havelsky [19] analyzed the problem of efficiency evaluation of systems for combined heat, cold and electricity production, and developed equations for energy efficiency and primary energy savings. The energy analysis of trigeneration plants with heat pumps was examined by Miguez et al. [20, 21]. They concluded that the heat pump is important for plant efficiency enhancement.

Khaliq et al. [9] carried out an exergy analysis of a combined electrical power and refrigeration cycle, as well as a parametric study of the effects of exhaust gas inlet temperature, pinch point and gas composition on energy and exergy efficiencies, electricity to cold ratio, and exergy destruction rate for a cogeneration system and its components. Cihan et al. [22] carried out energy and exergy analyses for a combined cycle located in Turkey and suggested modifications to decrease the exergy destruction in combined cycle power plants (CCPPs). Their results showed that combustion chambers, gas turbines and HRSGs are the main sources of irreversibilities, representing over 85 % of the overall exergy losses.

Barelli et al. [23] conducted an exergetic analysis of a residential CHP system based on a PEM fuel cell. They also conducted a complete parametric study to see the effect of fuel cell design parameters such as temperature, pressure and relative humidity on the system performance. Bingol et al. [24] reported the exergy based performance analysis of high efficiency polygeneration systems for sustainable building applications. El-Emam and Dincer [25] conducted the energy and exergy analyses of a CHP system with a molten carbonate fuel cell (MCFC) and a gas turbine system. They performed a parametric study by changing some design parameters of the system in order to assess the system performance. The results showed that the maximum output work of the MCFC is estimated to be 314 kW for an operating temperature of 650 °C. The overall energy and exergy efficiencies achieved for this system were 43 and 38 %, respectively.

Akkaya et al. [26] conducted the exergy analysis for a hybrid CHP system using a SOFC and a gas turbine and performed a parametric study. The results showed that a design based on an exergy performance coefficient criterion has considerable advantage in terms of entropy generation rate. Al-Sulaiman et al. [27] demonstrated an efficiency gain of more than 22 % using a trigeneration plant compared with a power cycle (SOFC and organic Rankine cycle). They also determined the maximum efficiencies of 74 % for the trigeneration plant, 71 % for heating cogeneration, 57 % for cooling cogeneration and 46 % for net electricity generation, and concluded that exergy analysis is a significant tool for both CHP and trigeneration cycles.

In recent decades, exergoeconomics and thermoeconomics have been increasingly utilized by researchers, combining thermodynamics with economics. Many such studies have been reported, especially for power generation and cogeneration (CHP). Rosen and Dincer [28] performed an exergoeconomic analysis of a coal fired electricity generating station, and found the ratio of thermodynamic loss rate to the capital cost to be a significant parameter in evaluating plant performance that

may allow thermodynamics and economics to be successfully traded-off in plant designs. Ahmadi et al. [29] carried out energy, exergy and exergoeconomic analyses of a steam power plant in Iran, and considered the effect of the load variations and ambient temperature on component exergy destruction rate. The results showed that energy losses are mainly associated with the condenser, where the energy loss rate to the environment was 307 MW, while the boiler energy loss rate was only 68 MW. However, the irreversibility rate of the boiler was significantly higher than the irreversibility rates of the other components. Exergy and exergoeconomic analyses of CHP plants [30–32] have demonstrated the usefulness of these methods for thermal systems.

Trigeneration Systems

Trigeneration commonly utilizes waste or other heat from a power plant to improve overall thermal performance, often utilizing the free energy available via waste energy. In a trigeneration system, waste heat from the plant's prime mover (e.g., gas turbine, diesel engine, or Rankine cycle [6]), sometimes with temperature enhancement, drives heating and cooling devices. The heat can be used for space heating, domestic hot water production, or to produce steam for process heating. The heat can also be used for cooling, by driving an absorption chiller. Pospisil et al. [33] performed an energy analysis of a trigeneration system and compared cogeneration and trigeneration plants for a typical building. The results showed that cogeneration can increase the efficiency by about 31 % while trigeneration systems increase efficiency by about 39% compared to a single generation system. Al-Sulaiman et al. [34] reported the performance comparison of three trigeneration systems using organic Rankine cycles. The systems they considered consist of SOFC-trigeneration, biomass-trigeneration, and solar-trigeneration. Martins et al. [35] studied the thermodynamic performance assessment of a trigeneration cycle considering the influence of operational variables. Calva et al. [36] studied the thermal integration of trigeneration systems. They focused on trigeneration schemes where a gas turbine is used as a prime mover for power production and cooling is generated by a typical compression refrigeration system. Huang et al. [37] reported a biomass fuelled trigeneration system in selected buildings. This trigeneration system consisted of an internal combustion (IC) engine integrated with biomass gasification. In their system the gas generated by the biomass gasifier was used to provide electricity for a typical building using an IC engine. The waste heat is then recovered from the engine cooling system and exhaust gases are utilized to supply hot water for space heating; excess heat was also used to drive an absorption cooling system.

Rocha et al. [38] studied the performance tests of two small trigeneration pilot plants. The first system was based on a 30 kW natural gas powered micro turbine, and the second used a 26 kW natural gas powered IC engine coupled with an electrical generator as a prime mover. They also used an ammonia water absorption refrigeration chiller for producing chilled water. Huicochea et al. [39] carried out a

thermodynamic analysis of a trigeneration system consisting of a micro gas turbine and a double effect absorption chiller. The system consisted of a microturbine to produce electrical power, a double effect absorption water LiBr chiller for air conditioning and a heat exchanger to produce hot water.

Chicco and Mancarella [40] proposed some energy indicators to assess the fuel efficiency of a trigeneration plant. Chicco and Mancarella [41] applied these energy indicators to introduce a planning criterion called equivalent gas price. Aghahosseini et al. [42] reported the thermodynamic analysis of an integrated gasification and Cu-Cl cycle for trigeneration of hydrogen, steam and electricity. They used Aspen HYSYS to simulate the system. The results showed that using oxygen instead of air for the gasification process, in which oxygen is provided by the integrated Cu-Cl cycle, led to a 20 % increase in the hydrogen content of produced syngas. Minciuc et al. [43] presented a method for analyzing trigeneration systems and established limits for the best performance of gas turbine trigeneration with absorption chilling from a thermodynamic point of view.

Moya et al. [44] studied the performance assessment of a trigeneration system consisting of a micro gas turbine and an air cooled, indirect fired, ammonia water absorption chiller. They also conducted a parametric study by changing some major design parameters, including variation of output power of the micro gas turbine, ambient temperature for the absorption unit, chilled water outlet temperature and thermal oil inlet temperature. Velumani et al. [45] proposed a new integrated trigeneration system consisting of a micro gas turbine, a solid oxide fuel cell and a single effect absorption chiller. The results showed that the energy efficiency of this cycle is about 70 %.

Buck and Fredmann [46] studied the performance of a trigeneration plant based on a micro turbine assisted by a small solar tower. They conducted an economic analysis on the use of single and double effect absorption chillers. The authors recommended using the double effect chiller since it showed better thermal performance and lower operating cost compared to the single effect absorption chiller.

Exergy is a useful tool for determining the location, type and true magnitude of exergy losses, which appear in the form of either exergy destructions or waste exergy emissions [47]. Therefore, exergy can assist in developing strategies and guidelines for more effective use of energy resources and technologies. Recently, exergy analysis has become increasingly popular for analyzing thermal systems. Some studies have applied exergy analyses to CHP and trigeneration energy systems based on IC engines. Santo et al. [48] conducted the energy and exergy analyses of a IC engine based trigeneration system under two operating strategies for buildings. They presented a computational hourly profile method that combined fittings from the literature and actual data from manufacturer into a single algorithm curve in order to obtain the mathematical representations of physical phenomena and thermodynamic properties. The developed simulation method was used to predict the performance of a given cogeneration concept under two operational strategies.

Ebrahimi et al. [49] carried out energy and exergy analyses of a micro steam CCHP cycle for a residential building. They analyzed a trigeneration energy system consisting of a steam turbine and an ejector refrigeration system to provide

the cooling load for residential buildings. They also optimized the system using a genetic algorithm to determine its maximum overall efficiency. The exergy analysis results revealed that the greatest exergy destruction rate takes place in the steam generator for both summer and winter seasons.

Khaliq [50] conducted an exergy analysis for a trigeneration system. The system studied consisted of a gas turbine cycle, a single pressure heat recovery steam generator to provide heating and a single effect Li-Br absorption chiller to provide sufficient cooling. He also conducted a comprehensive parametric study to investigate the effects of compressor pressure ratio, gas turbine inlet temperature, combustion chamber pressure drop, and evaporator temperature on the exergy destruction rate in each component, first law efficiency, electrical to thermal energy ratio, and second law efficiency of the system. The exergy analysis results indicated that that maximum exergy destruction rate occurred in the combustion and steam generation process, which represented over 80 % of the total exergy destruction rate in the overall system.

Kong et al. [51] conducted energy and economic analyses of a trigeneration plant using a Stirling engine as a prime mover with a conventional plant with a separate production of cooling, heating and power. They concluded that the trigeneration plant with the Stirling engine can save more than 33 % of the primary energy compared to the conventional plant. Ziher and Poredos [52] addressed the economics of using a trigeneration plant in a hospital. They calculated the cooling, heating, and power price per kWh on a monthly basis for 1 year. In order to obtain the cooling capacity, the authors suggested that the use of steam absorption and compression chillers with a cold storage system in the plant. Ahmadi et al. [6] carried out an exergoenvironmental analysis of a trigeneration system based on a micro gas turbine and an organic Rankine cycle (ORC), and performed a parametric study involving the main design parameters of the trigeneration system.

Temir and Bilge [53] studied a thermoeconomic analysis of a trigeneration system that produces electrical power with a natural gas fed reciprocating engine and that yields absorption cooling by making use of the system's exhaust gases. Ehyaei and Mozafari [54] performed energy, economic and environmental impact assessment ofa micro gas turbine employed for on-site combined heat and power production, and examined the optimization of the micro turbine application to meet the electrical, heating and cooling loads of a building. Mago and Hueffed [18] evaluated a turbine driven combined cooling, heating and power (CCHP) system for large office buildings under various operating strategies, and explored the use of carbon credits to show how the possible reduction in carbon dioxide emissions via a CCHP system could translate into economic benefits. Ozgener et al. [55] developed an exergoeconomic model for a vertical ground source heat pump (GSHP) residential heating system. They calculated the ratio of thermodynamic loss rate to capital cost values to be in the range of 0.18–0.43, and provided a linear correlation between the value of this parameter and ambient temperatures. They also drew attention to the compressor as the component where the most exergy destruction occurred.

Ozgener and Hepbasli [56] conducted an exergoeconomic analysis for a solar assisted ground source heat pump heating system with a 50 m vertical and 32 mm

nominal diameter U bend ground heat exchanger. They determined that the total exergy loss values were between 0.010and 0.480 kW and found the largest energy and exergy losses in the greenhouse compressor. Moreover, they have calculated the ratio of thermodynamic loss rate to capital cost values to be in the range of 0.035–1.125.

Many reports in the literature consider environmental aspects of thermal systems. Dincer [57] and Dincer and Rosen [47] considered the environmental and sustainability aspects of hydrogen and fuel cell systems. The exergetic and environmental aspects of drying systems have also been examined [17]. Ahmadi and Dincer [4] conducted an exergoenvironmental optimization of a CHP system using a genetic algorithm, and a sensitivity analysis of how optimized design parameters vary with the fuel cost. A thermodynamic analysis of post-combustion CO_2 capture in a natural gas fired power plant has been reported by Amrolahi et al. [58]. Petrakopoulou et al. [59] studied exergoeconomic and exergoenvironmental analyses of a combined cycle power plant with chemical looping technology. This research provided an evaluation of chemical looping combustion technology from an economic and environmental perspective by comparing it with a reference plant, a combined cycle power plant that includes no CO_2 capture.

For various reasons, it is important to optimize processes so that an objective function is maximized or minimized. For example, the output, profit, productivity, product quality, etc., may be maximized, or the cost per item, investment, energy input, etc., may be minimized. The success and growth of industries today is strongly based on their ability to optimize designs and systems. With the advent in the recent years of new materials, such as composites and ceramics, and new manufacturing processes, several traditional industries (e.g., steel) have faced significant challenges and, in some cases, diminished in size, while many new fields have emerged. It is important to exploit new techniques for product improvement and cost reduction in traditional and new industries. Even in an expanding area, such as consumer electronics, the prosperity of a company is closely connected to its ability to apply optimization to new and existing process and system designs. Consequently, engineering design, which has always been important, has become increasingly coupled with optimization [47].

Energy engineering is a field where optimization plays a particularly important role. Engineers involved in thermal energy engineering, for instance, are required to answer the questions such as

- What processes or equipment should be selected for a system, and how should the parts be arranged for the best outcome?
- What are the best characteristics for the components (e.g., size, capacity, cost)?
- What are the best process parameters (e.g., temperature, pressure, flow rate and composition) of each stream interacting with the system?

In order to answer such questions, engineers are required to formulate an appropriate optimization problem. Proper formulation is usually the most important and sometimes the most difficult step in optimization. To formulate an optimization problem, there are numerous elements that need to be defined, including system boundaries, optimization criteria, decision variables and objective functions.

Sahoo [60] carried out an exergoeconomic analysis and optimization of a cogeneration system which produces 50 MW of electricity and 15 kg/s of saturated steam at 2.5 bar. He optimized the unit using exergoeconomic principles and evolutionary programming, and showed that the cost of electricity production is 9.9% lower for the optimum case in terms of exergoeconomics compared to a base case. Sayyaadi and Sabzaligol [61] performed an exergoeconomic optimization of a 1000 MW light water nuclear power generation system using a genetic algorithm and considering ten decision variables, and showed that the fuel cost of the optimized system is greater than that for a base case. Shortcomings in the optimized system are compensated by larger monetary savings in other economic sectors. Haseli et al. [62] found the optimum temperatures in a shell and tube condenser with respect to exergy. The optimization problem in that study considered condensation of the entire vapor flow and was solved with sequential quadratic programming (SQP).

Saayaadi and Nejatolahi [63] analyzed cooling tower assisted vapor compression refrigeration machines with respect to total exergy destruction rate and total product cost objective functions. They used energy and exergy analyses for the thermodynamic model and incorporated Total Revenue Requirement (TRR) for the economic model. They have optimized the system with respect to single objective thermodynamic, single objective economic and multi-objective criteria. For the multi-objective optimization, they selected final solutions from the Pareto frontier curve. Finally, they compared the results obtained from the three optimizations and calculated that the percentage deviation from ideal results for thermodynamic and economic criteria is 40% for thermodynamically optimized system, 83% for economically optimized system and 23% for the multi-objective optimized system and therefore determined that the multi-objective optimization satisfies the generalized engineering criteria more than the other two single-objective optimized designs.

Ahmadi et al. [64] conducted a comprehensive exergy, exergoeconomic and environmental impact analyses and a multi-objective optimization for combined cycle power plants (CCPPs) with respect to the exergy efficiency, total cost rate and CO_2 emissions of the overall plant. They determined that the largest exergy destructions occurred in the CCPP combustion chamber and that increasing the gas turbine inlet air temperatures decreases the CCPP cost of exergy destruction. They derived the expression for the Pareto optimal point curves for the determined exergy efficiency range and concluded that the increase in total cost per unit exergy efficiency is considerably high after exergy efficiencies over 57% and therefore a point below this should be chosen on the Pareto optimal curve.

Sayyaadi and Babaelahi [65] analyzed a liquefied natural gas re-liquefaction plant with respect to multi-objective approach which simultaneously considers exergy and exergoeconomic objectives. They used MATLAB multi-objective optimization algorithm of NSGA-II, which is based on the Genetic Algorithm, and obtained Pareto optimal frontier to find the Pareto optimal solutions. They compared the final optimal system with the base case and found that the exergetic efficiency in the multi-objective optimum design is 11% higher than that of the exergoeconomic optimized system, while the total product cost of the multi-objective optimal design is 16.7% higher than that of the exergoeconomic optimal system.

Ghaebi et al. [66] conducted the exergoeconomic optimization of a trigeneration system for heating, cooling and power production purpose based on total revenue requirement (TRR) method and using evolutionary algorithm. The system studied consists of an air compressor, a combustion chamber, a gas turbine, a dual pressure heat recovery steam generator and an absorption chiller in order to produce cooling, heating and power. The economic model used in their research was the TRR and the cost of the total system product was defined as our objective function and optimized using a genetic algorithm technique.

Kavvadias and Maroulis [67] investigated the multi-objective optimization of a trigeneration plant. This optimization was carried out on technical, economical, energetic and environmental performance indicators in a multi-objective optimization framework. The results showed that trigeneration plants can be more economically attractive, energy efficient and environmental friendly than conventional cogeneration plants. Al-Sulaiman et al. [68] studied the thermoeconomic optimization of three trigeneration systems using organic Rankine cycles. The three systems considered were SOFC-trigeneration, biomass-trigeneration, and solar-trigeneration systems. The results showed that solar based trigeneration system has the highest net available exergy as compared to the other two systems. Therefore, it has the highest potential to have the highest exergy if the solar collector performance is improved.

Wang et al. [69] conducted multi-objective optimization of an organic Rankine cycle (ORC) for low grade waste heat recovery using evolutionary algorithm. The multi-objective optimization of the ORC with R134a as the working fluid was conducted in order to achieve the system optimization design from both thermodynamic and economic aspects using non-dominated sorting genetic algorithm (NSGA-II). The decision variables considered for multi-objective optimization were turbine inlet pressure, turbine inlet temperature, pinch temperature difference, approach temperature difference and condenser temperature difference are selected as the decision variables.

Shirazi et al. [70] conducted a comprehensive thermodynamic modeling and multi-objective optimization of an internal reforming solid oxide fuel cell gas turbine hybrid system. They validated the model using available data in the literature. They used genetic algorithm to optimize the system. In the multi-objective optimization procedure, the exergy efficiency and the total cost rate of the system (including the capital and maintenance costs, operational cost and social cost of air pollution for CO, NO_x, and CO_2) were considered as objective functions. They also performed sensitivity analyses of the variation of each objective function with major design parameters of the system.

Multigeneration Energy Systems

Hosseini et al. [71] conducted a comprehensive thermodynamic model for an integrated energy system. The system studied consists of a gas turbine, a SOFC fuel cell, a single pressure HRSG and a multi effect desalination to produce electricity,

heating, cooling and fresh water. They also performed a comprehensive parametric study to see the effect of some major design parameters on the system performance. The results showed that the integrated system could increase the system efficiency by about 25 % compared to a single generation system.

Ahmadi et al. [6] studied a new integrated trigeneration energy system consisting of a gas turbine, a double pressure heat recovery steam generator and a single effect absorption chiller and an organic Rankine cycle. They also performed a parametric study to see the variation of exergy efficiency, cooling and heating load and cost of environmental impact. The results of this study demonstrated that system performance is notably affected by the compressor pressure ratio, the gas turbine inlet temperature and the gas turbine isentropic efficiency.

Ratlamwala et al. [72] studied a performance assessment of an integrated PV/T and triple effect cooling system for hydrogen and cooling production. The also conducted a comprehensive parametric study on the effect of average solar radiation for different months, operating time of the electrolyzer, inlet air temperature and PV area module on the power production and hydrogen production rate. In another study, Ratlamwala et al. [73] analyzed the performance of a novel integrated geothermal system for multigeneration, based on a geothermal double flash power generating unit, an ammonia water quadruple effect absorption unit and an electrolyzer system for cooling, heating, power, hot water and hydrogen production. Increasing the geothermal source temperature, pressure and mass flow rate was observed to increase the output power and hydrogen production rate.

Ozturk and Dincer [74] conducted a thermodynamic analysis of a solar based multigeneration system with hydrogen production. The solar based multigeneration considered for this analysis consists of four main sub systems: Rankine cycle, organic Rankine cycle, absorption cooling and heating, and hydrogen production and utilization. The exergy efficiency and exergy destruction rate for the subsystems and the overall system show that the parabolic dish collectors have the highest exergy destruction rate among constituent parts of the solar-based multigeneration system.

Dincer and Zamfirescu [7] performed energy and exergy analyses of renewable-energy-based multigeneration, considering several options for producing such products as electricity, heat, hot water, cooling, hydrogen, and fresh water. Ahmadi et al. [75] studied the exergo-environmental analysis of an integrated organic Rankine cycle for polygeneration to produce electricity, heating, cooling and hot water. The system analyzed consists of a gas turbine cycle, an organic Rankine cycle (ORC), a single effect absorption chiller and a domestic water heater. The exergy efficiency of the trigeneration system is found to be higher than that of typical combined heat and power systems or gas turbine cycles. The results also indicate that carbon dioxide emissions for the trigeneration system are less than for the aforementioned systems. The exergy results show that combustion chamber has the largest exergy destruction of the cycle components, due to the irreversible nature of its chemical reactions and the high temperature difference between the working fluid and flame temperature.

Ahmadi et al. [76] studied a thermodynamic modeling and assessment of an integrated biomass-based multigeneration energy system. They analyzed a new multigeneration system based on a biomass combustor, an organic Rankine cycle (ORC), an absorption chiller and a proton exchange membrane electrolyzer to produce hydrogen, and a domestic water heater for hot water production, is proposed and thermodynamically assessed. Also, they conducted exergy analysis to determine the irreversibilities in each component and the system performance. In addition, an environmental impact assessment of the multigeneration system was performed, and the potential reduction in CO_2 emissions when the system shifts from power generation to multigeneration are investigated.

Ahmadi et al. [8] carried out an exergy-based optimization of a multigeneration energy system. They considered a multigeneration energy system with a gas turbine as the prime mover to produce electricity, heating, cooling and domestic hot water, and applied a multi-objective evolutionary based optimization to find the best design parameters of the system considering exergy efficiency and total cost of the system as two objective functions.

The research reported to date suggests that multigeneration is often advantageous for mitigating global warming and increasing efficiency. However, complete energy, exergy, and environmental impact assessments of a multigeneration based on micro gas turbine and ejector refrigeration system, biomass based multigeneration system and ocean thermal energy conversion based multigeneration system have not been reported in the literature. Also, a fast and elitist non-dominated sorting genetic algorithm (NSGA-II) based multi-objective optimization for such complex systems has not been used yet in such research.

6.3 Descriptions of Case Studies

In this section, three novel multigeneration energy systems are modeled, analyzed and compared. The system products include electricity, heating, cooling, hot water, fresh water and hydrogen, and various sources of energy are considered like heat source from conventional to renewable energy sources.

Case study I: Multigeneration System Based on Gas Turbine Prime Mover

A gas turbine is mature and advantageous prime mover for many reasons, so it is used in one of the multigeneration energy systems considered here. This system is comprised of five subsystems (see Fig. 6.6).Electricity is produced by a gas turbine and a steam turbine while cooling is produce based on two different cycles, a single effect absorption chiller and an ejector refrigeration cycle. To produce hydrogen, a

PEM electrolyzer is used driven by electricity produced by the ejector. A domestic water heater uses the energy from the absorption generator. A more complete explanation of each subsystem is given below.

Figure 6.6 illustrates an integrated multigeneration system containing a compressor, a combustion chamber (CC), a gas turbine, a double pressure heat recovery steam generator (HRSG) to produce superheated steam, a single effect absorption chiller, a heat recovery vapor generator (HRVG) to produce ORC vapor that is driven by heat from flue gases from the HRSG, an organic Rankine cycle (ORC) ejector refrigeration system, a PEM electrolyzer for hydrogen production and a domestic water heater for hot water production. Air at ambient conditions enters the air compressor at point 1 and exits after compression (point 2). The hot air enters the combustion chamber (CC) into which fuel is injected, and hot combustion gases exit (point 3) and pass through a gas turbine to produce shaft power. The hot gas expands in the gas turbine to point 4. Hot flue gases enter the double pressure HRSG to provide high and low pressure steam at points 5 and 14. High pressure steam enters the steam turbine to generate shaft power while the low pressure steam enters the generator of the absorption system to provide the cooling load of the system. The low pressure line leaving the generator has adequate energy for use in a domestic water heater that provides hot water at 50 °C. Furthermore, flue gases leaving the HRSG at point *C* enter a heat recovery vapor generator to provide electricity and cooling. Since the flue gases have a low temperature, around 160 °C, an ORC cycle is used, consisting of an ORC turbine to generate electricity and a steam ejector to provide the system cooling load. These flue gases enter the HRVG at point *d* to produce saturated vapor at point 29, which leaves the HRVG at point 28. Saturated vapor at point 29 enters the ORC turbine and work is produced. The extraction turbine and ejector play important roles in this combined cycle. The high pressure and temperature vapor is expanded through the turbine to generate power, and the extracted vapor from the turbine enters the supersonic nozzle of the ejector as the primary vapor. The stream exiting the ejector (point 33) mixes with turbine exhaust (point 31) and is cooled in the preheater and enters the condenser where it becomes a liquid by rejecting heat to the surroundings. Some of the working fluid leaving the condenser enters the evaporator after passing through the throttle valve (point 39), and the remainder flows back to the pump (point 37). The ORC pump increases the pressure (point 40), and high pressure working fluid is heated in the preheater (point 41) before entering the HRVG. The low pressure and temperature working fluid after the valve (point 39) enters the evaporator, providing a cooling effect for space cooling. Some of the electricity is considered for residential applications while some directly drives a PEM electrolyzer to produce hydrogen. In this analysis, waste heat is used as a heat source to stimulate the multigeneration system and R123 is selected as the working fluid because it is a non-toxic, non-flammable and non-corrosive refrigerant with suitable thermophysical characteristics.

Case study II: Biomass Based Multigeneration System

Renewable energy is a source of energy which comes from natural resources such as sunlight, wind, rain, tides, waves, geothermal heat and biomass. These are naturally replenished when used. Biomass, as a renewable energy source, is biological material from living, or recently living, organisms [77].

Comprehensively, biomass comprises all the living matter present on Earth and, as an energy source, biomass can either be used directly, or converted into other energy products such as biofuels [77]. Currently, biomass resources are mainly used in the production of heating, cooling and electricity. Direct combustion of biomass with coal is the most common method of conversion and provides the greatest potential for large scale utilization of biomass energy in the near term [78]. Other thermochemical conversion technologies such as gasification and pyrolysis are technically feasible and potentially efficient, compared to combustion, for power generation. However, these technologies either lack of maturity and reliability or are not economically viable for large scale utilization [79]. Biomass based cogeneration systems are studied over many years by numerous researchers for various industries (e.g., sugar, rice, palm oil, paper and wood) as a means of waste disposal and energy recovery [80].

Figure 6.7 illustrates an integrated multigeneration system containing a biomass combustor, an ORC cycle to produce electricity, a double-effect absorption chiller for cooling, a heat exchanger for heating, a proton exchange membrane (PEM) electrolyzer to produce hydrogen, a domestic water heater to produce hot water and a reverse osmosis (RO) desalination to produce fresh water. Pine sawdust is used as the biomass fuel and burned in a biomass combustor. The heat from the biomass combustor is input to the ORC cycle. The waste heat from the ORC is utilized to produce steam in the heating process via the heat exchanger, and to produce cooling using a double-effect absorption chiller. To have an efficient ORC, its working fluid should have a high critical temperature so that the waste heat can be used more efficiently [75]. A typical organic fluid used in ORCs is n-octane, which has a relatively high critical temperature (569 K) [76]. This organic fluid is selected here as the working fluid of the ORC. The ORC cycle produces electricity, part of which is used for residential applications depending on electricity needs of the building, and the remainder of which drives a PEM electrolyzer for hydrogen production and RO desalination to produce fresh water. The hydrogen and fresh water are stored in a hydrogen tank and fresh water tank respectively. Since the flue gases leaving the ORC evaporator still have energy, they are utilized to produce hot water in a domestic water heater.

As shown in Fig. 6.7 biomass enters the combustor at point 30 and air enters at point 29. Hot flue gases leave the biomass combustor at point 31 and then enter a cyclone to remove the ash. Hot flue gases without ash enter an ORC evaporator to produce steam at point 27 to rotate the ORC turbine blades and produce shaft work. The high-pressure and temperature vapor at point 27 is expanded through the turbine to generate power, and the extracted vapor from the turbine enters the heat exchanger for the heating process. Saturated vapor leaves the heating process unit

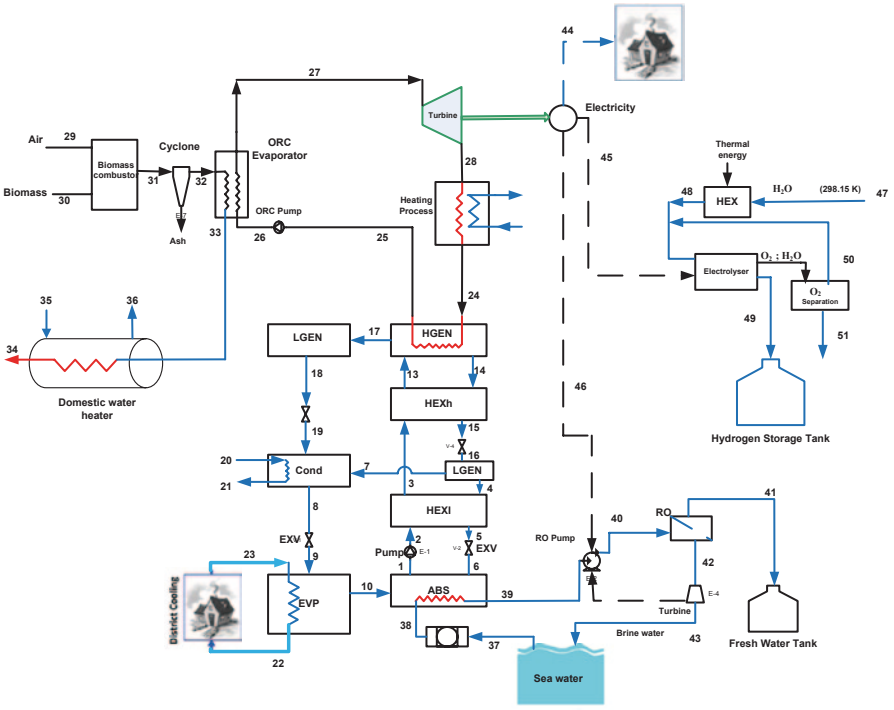

Fig. 6.7 Schematic of biomass based a multigeneration energy system for the provision of heating, cooling, electricity, hydrogen, fresh water and hot water [5]

at point 24. This saturated steam enters the generator of the double-effect absorption system to provide the cooling load of the system. Saturated liquid leaves the absorption generator and enters the ORC pump at point 25. ORC pump increase the pressure of ORC working fluid and high pressure ORC fluid enters the ORC evaporator at point 26 to close the ORC power generation unit. Since flue gases leaving the ORC evaporator still have energy, a domestic water heater is used to utilize the energy of the hot gases at point 33. Water enters the domestic water heater at point 35 and hot water leave the domestic water heater at point 36. Reverse osmosis (RO) desalination is used to produce fresh water as shown right bottom side of Fig. 6.9.

Sea water at point 37 enters a filter to remove dissolved species and then passes through the absorber of the double-effect absorption chiller to increase the temperature to improve the efficiency of the OR desalination unit. A high pressure RO pump is used to increase the pressure of the water. High pressure sea water leaves the RO pump and enters the RO unit at point 40. Fresh water is produced at point 41 and stored in a fresh water tank for the later use while high pressure brine water enters a hydraulic turbine to reduce the pressure and generate electricity. Finally, low pressure brine water leaves the RO unit and sends back to the sea. The cooling load of the system is provided by a double-effect absorption chiller. Weak Li-Br solution at point a is pumped through an high pressure solution leaves the pump at point 2 then

passes through a high temperature heat exchanger to increase the temperature. High temperature weak solution then enters the high temperature heat exchanger at point 3 and the high temperature weak solution enters the high temperature generator. In high temperature generator water is removed from the solution and the strong solution sends back to the absorber after passing through the high and low temperature heat exchangers. On the other side, vapor leaves the high temperature generator at point 17 and enters the low temperature generator. The refrigerant steam produced by the low pressure generator is condensed by the cooling water and then enters the expansion valve at point 8 to reduce the pressure and enters the evaporator at point 9. This low pressure vapor enters the evaporator and saturated vapor leaves the evaporator at point 10 and enters the absorber. The absorption heat is removed by the sea water entering the absorber at point 38 to improve the efficiency of the RO desalination unit.

Case Study III: Integrated Ocean Thermal Energy Conversion Multigeneration System

A large amount of solar energy is stored as heat in the surface waters of the world's oceans, providing a source of renewable energy. Ocean thermal energy conversion (OTEC) is a process for harnessing this renewable energy in which a heat engine operates between the relatively warm ocean surface, which is exposed to the sun, and the colder (about 5 °C) water deeper in the ocean, in order to produce electricity. OTEC usually incorporates a low-temperature Rankine cycle engine which boils a working fluid such as ammonia to generate a vapor which turns the turbine to generate electricity, and then is condensed back into a liquid in a continuous process. 80 % of the energy that is received from the sun by the earth is stored in the world's oceans [81, 82], and many regions of the world have access to this OTEC resource. OTEC can produce fuels by using its product electricity to produce hydrogen, which can be used in hydrogen fueled cars as well as in the development of synthetic fuels. For a small city, millions of tons of CO_2 are generated annually through fossil fuel use while with OTEC the value is zero, during the operation of devices. OTEC has a potential to replace some fossil fuel use, perhaps via OTEC ships travelling the seas of the world.

An OTEC system utilizes low-grade energy and has a low energy efficiency (approximately 3–5 %). Therefore, achieving a high electricity generating capacity with OTEC requires the use of large quantities of seawater, and a correspondingly, large amounts of pumping power. These factors have negative impact on the cost-effectiveness of this technology and therefore OTEC is not commercially viable today. In order to improve the effectiveness and economics of OTEC cycles, it is proposed to integrate them with industrial operations so that, apart from generating electricity, they could be used for fresh water production, air conditioning and refrigeration, cold water agriculture, aquaculture and mariculture, and hydrogen

production [81]. Potential markets for OTEC have been identified, most of which are in the Pacific Ocean, and about 50 countries are examining its implementation as a sustainable source of energy and fresh water, including India, Korea, Palau, Philippines, the U.S. and Papua New Guinea [83]. In 2001, as a result of cooperation between Japan and India, a 1-MW OTEC plant was built in India [83], and others are planned to be constructed in the near future [84].

Considerable research has been directed to the development of OTEC recently. Uehara [85–87] conducted numerous theoretical and experimental studies on the major components of an OTEC plant, and showed that ammonia is a suitable working fluid for an OTEC plant employing a closed organic Rankine cycle (ORC). The energy efficiency of the Rankine cycle in an OTEC plant is usually limited to around 5 % due to the small temperature differences between surface water and deep water of the ocean. Thus, in order to improve the efficiency of OTEC, other thermodynamic cycles such as the Kalina cycle and the Uehara cycle that use an ammonia–water mixture as the working fluid are being considered [88]; they are reported to have better energy efficiencies than a Rankine cycle at the same temperature difference [88]. Increasing in the temperature difference between the hot heat source and the cold heat sink can improve the efficiency of OTEC plants, as can the integration of OTEC with other energy technologies. Saitoh and Yamada [88] proposed a conceptual design of a multiple Rankine-cycle system using both solar thermal energy and ocean thermal energy in order to improve the cycle efficiency.

Figure 6.8 shows a schematic diagram of an integrated OTEC system equipped with a flat plate and PV/T solar collector, a reverse osmosis (RO) desalination unit, a single effect absorption chiller and PEM electrolyzer. This integrated system uses the warm surface seawater to evaporate a working fluid such as ammonia or a Freon refrigerant, which drives an ORC turbine to produce electricity, which in turn is used to drive a PEM electrolyzer to produce hydrogen. After passing through the turbine, the vapor is condensed in a heat exchanger that is cooled by cold deep seawater. The working fluid is then pumped back through the warm seawater heat exchanger, and the cycle is repeated continuously. Warm surface water is pumped from the ocean surface at point 1. A warm surface pump increases the pressure where the high pressure warm water enters a flat plate collector at point 2 to increase its temperature. Water enters an evaporator at point 3 and after a heat exchange with the ORC fluid, leaves the evaporator at point 4 where it is flushed back to the ocean surface.

A PV/T solar panel is considered to provide the cooling load of the system. Air enters the PV/T panel at point 41 and, after absorbing the sun's heat using its panels, its temperature increases. Next, the hot air leaves the PV/T at point 40 and enters the absorption chiller generator in order to run the chiller. The electricity generated by PV/T is directed to derive a RO desalination plant to produce fresh water. In this multigeneration system, a provision of the electricity generated by OTEC plant is used to produce hydrogen using a PEM electrolyzer at point 22. The produced hydrogen is stored in a hydrogen storage tank for later usage.

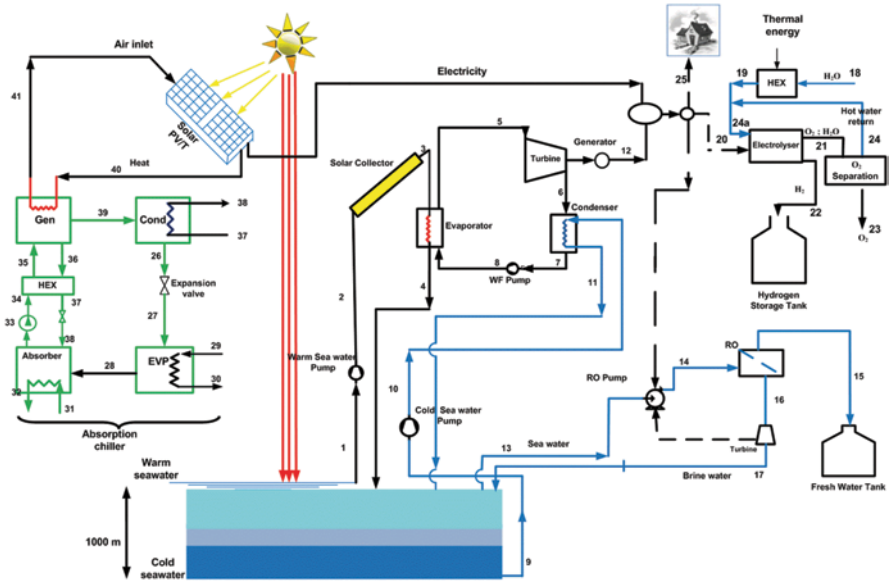

Fig. 6.8 Schematic of an integrated renewable based multigeneration energy system for the provision of cooling, electricity, hydrogen, fresh water [5]

6.4 Exergy Analyses

Exergy analysis can help develop strategies and guidelines for more efficient and effective use of energy, and is utilized to study various thermal processes, especially power generation, CHP, trigeneration and multigeneration. The exergy of a substance is often divided into four components. Two common ones are physical and chemical exergy. The two others, kinetic and potential exergy, are assumed to be negligible here, as elevation changes are small and speeds are relatively low [29, 47, 76]. Physical exergy is defined as the maximum useful work obtainable as a system interacts with an equilibrium state. Chemical exergy is associated with the departure of the chemical composition of a system from its chemical equilibrium and is considered important in processes involving combustion and other chemical changes [88–90]. Through the second law of thermodynamics, the following exergy rate balance is written as

$$\dot{E}x_Q + \sum_i \dot{m}_i ex_i = \sum_e \dot{m}_e ex_e + \dot{E}x_W + \dot{E}x_D \tag{6.1}$$

where subscripts i and e denote the control volume inlet and outlet flow, respectively, $\dot{E}x_D$ is the exergy destruction rate and other terms are given as follows:

$$\dot{E}x_Q = \left(1 - \frac{T_0}{T_i}\right)\dot{Q}_i \tag{6.2}$$

$$\dot{E}x_w = \dot{W} \tag{6.3}$$

$$ex = ex_{ph} + ex_{ch} \tag{6.4}$$

Here, $\dot{E}x_Q$ is the exergy rate of heat transfer crossing the boundary of the control volume at absolute temperature T, the subscript 0 refers to the reference environment conditions and $\dot{E}x_W$ is the exergy rate associated with shaft work. Also, ex_{ph} is defined as follows:

$$ex_{ph} = (h - h_0) - T_0(s - s_0) \tag{6.5}$$

The specific chemical exergy for gas mixtures is defined as follows [90]:

$$ex_{mix}^{ch} = \left[\sum {}_{i=1}^{n} x_i ex_i^{ch} + RT_0 \sum {}_{i=1}^{n} x_i \ln x_i\right] \tag{6.6}$$

The above equation cannot be used to evaluate fuel exergy. Here, fuel exergy is approximated with the following simplification [29, 90]:

$$\xi = \frac{ex_f}{LHV_f} \tag{6.7}$$

The ratio of chemical exergy to LHV_f is usually close to unity for common gaseous fuels, e.g., $\xi_{CH_4} = 1.06$, $\xi_{H_2} = 0.985$

For a general gaseous fuel with composition C_xH_y, the following experimental correlation can be used for ξ [90]:

$$\xi = 1.033 + 0.0169\frac{y}{x} - \frac{0.0698}{x} \tag{6.8}$$

Exergy Analysis of System I

Here, the exergy of each flow is calculated at all states and the changes in exergy are determined for each major component. The exergy destructions for all components in this multigeneration system are shown in Table 6.1. Since in this multigeneration energy system, a combustion reaction occurs in combustion chamber, it is important to calculate the chemical exergy where combustion takes place and where the solution is not real such as LiBr solution. Chemical exergy is equal to the maximum amount of work that can be obtained when a substance is brought from the reference-environment state to the dead state by a process including heat transfer and exchange of substances only with the reference environment. The maximum work

Table 6.1 Expressions for exergy destruction rates for components of system I

Component	Exergy destruction rate expression
Air compressor	$\dot{E}x_{D,AC} = \dot{E}x_1 - \dot{E}_2 - \dot{W}_{AC}$
Combustion chamber (CC)	$\dot{E}x_{D,CC} = \dot{E}x_2 + \dot{E}x_f - \dot{E}x_3$
Gas turbine (GT)	$\dot{E}x_{D,GT} = \dot{E}x_3 - \dot{E}x_4 - \dot{W}_{GT}$
HRSG	$\dot{E}x_{D,HRSG} = \dot{E}x_4 + \dot{E}x_8 - \dot{E}x_5 - \dot{E}x_c$
Steam turbine (ST)	$\dot{E}x_{D,ST} = \dot{E}x_5 - \dot{E}x_6 - \dot{W}_{ST}$
Steam condenser	$\dot{E}x_{D,Cond} = \dot{E}x_6 + \dot{E}x_{49} - \dot{E}x_7 - \dot{E}x_{50}$
Pump	$\dot{E}x_{D,P} = \dot{E}x_7 - \dot{E}x_8 + \dot{W}_P$
Heat recovery vapor generator	$\dot{E}x_{D,HRVG} = \dot{E}x_c + \dot{E}x_{41} - \dot{E}x_{28} - \dot{E}x_{29}$
ORC turbine	$\dot{E}x_{D,ORCT} = \dot{E}x_{29} - \dot{W}_{ORC} - \dot{E}x_{30} - \dot{E}x_{31}$
Ejector	$\dot{E}x_{D,Ejector} = \dot{E}x_{30} + \dot{E}x_{32} - \dot{E}x_{33}$
Preheater	$\dot{E}x_{D,PRH} = \dot{E}x_{34} + \dot{E}x_{40} - \dot{E}x_{35} - \dot{E}x_{41}$
ORC pump	$\dot{E}x_{D,ORCPump} = \dot{E}x_{37} + \dot{W}_{ORC} - \dot{E}x_{40}$
ORC condenser	$\dot{E}x_{D,Cond} = \dot{E}x_{35} - \dot{E}x_{36} - \dot{E}x_{Q,Cond}$
ORC evaporator	$\dot{E}x_{D,EVP} = \dot{E}x_{39} + \dot{E}x_{40} - \dot{E}x_{32} - \dot{E}x_{41}$
ORC expansion valve	$\dot{E}x_{D,EXV} = \dot{E}x_{38} - \dot{E}x_{39}$
Domestic water heater	$\dot{E}x_{D,DWH} = \dot{E}x_{15} + \dot{E}x_{17} - \dot{E}x_{16} - \dot{E}x_{18}$
PEM electrolyzer	$\dot{E}x_{D,PEM} = \dot{E}x_{42} + \dot{W}_{PEM} - \dot{E}x_{46} - \dot{E}x_{47} + \dot{E}x_Q$
Absorption condenser	$\dot{E}x_{D,Cond} = \dot{E}x_{19} - \dot{E}x_{20} - \dot{E}x_Q$
Absorption expansion valve	$\dot{E}x_{D,EXV} = \dot{E}x_{20} - \dot{E}x_{21}$
Absorption evaporator	$\dot{E}x_{D,EVP} = \dot{E}x_{21} - \dot{E}x_{22} + \dot{E}x_Q$
Absorber	$\dot{E}x_{D,Abs} = \dot{E}x_{22} + \dot{E}x_{23} - \dot{E}x_{25} - \dot{E}x_Q$
Absorption pump	$\dot{E}x_{D,P} = \dot{E}x_{25} + \dot{W}_P - \dot{E}x_{26}$
Absorption heat exchanger	$\dot{E}x_{D,HEX} = \dot{E}x_{26} + \dot{E}x_{14'} - \dot{E}x_{24} - \dot{E}x_{27}$
Absorption generator	$\dot{E}x_{D,Gen} = \dot{E}x_{14} + \dot{E}x_{27} - \dot{E}x_{15} - \dot{E}x_{14'} - \dot{E}x_{19}$

is attained when the process is reversible. Alternatively, chemical exergy can also be viewed as the exergy of a substance that is at the reference-environment state.

Chemical exergy is also equivalent to the minimum amount of work necessary to produce a substance at the reference-environment state from the constituents in the reference environment. Chemical exergy has two main parts, reactive exergy resulting from the chemical reactions necessary to produce species which do not exist as stable components in the reference environment, and concentration exergy resulting from the difference between the chemical concentration of a species in a system and its chemical concentration in the reference environment [47]. The concentration part is related to the exergy of purifying or diluting a substance, such as separating oxygen from air.

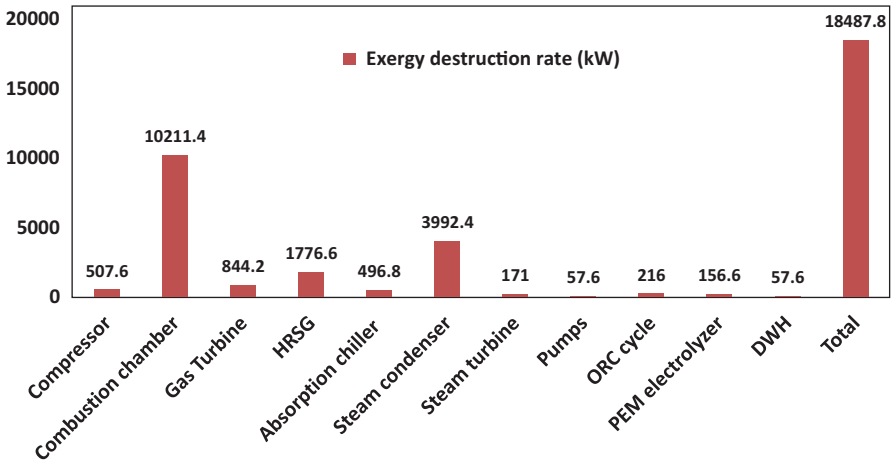

Fig. 6.9 Exergy destruction rates for the gas turbine multigeneration system and its components

As shown in Fig. 6.9, combustion reaction occurs in combustion chamber where the energy of fuel is converted to increase the temperature at gas turbine inlet temperature. Since chemical component of the gasses leaving the combustion chamber differ from the one in the reference environment, we should use chemical exergy of mixture to calculate the chemical exergy at at point 3 in Fig. 6.6.Therefore, we should first define the partial pressures and molar fractions of various constituents of air.

Exergy Analysis of System II

Here, the exergy of each flow is calculated at all states and the changes in exergy are determined for each major component. The exergy destructions for all components in this multigeneration system (Fig. 6.7) are listed in Table 6.2.

The exergy efficiency, defined as the product exergy output divided by the exergy input [47], can be expressed for the ORC power generation unit, the CHP unit and the multigeneration system as follows:

$$\psi_{ORC} = \frac{\dot{W}_{net,ORC}}{\dot{E}x_{biomass}} \tag{6.9}$$

$$\psi_{CHP} = \frac{\dot{W}_{net,ORC} + \dot{E}x_{heating}}{\dot{E}x_{biomass}} \tag{6.10}$$

$$\psi_{multi} = \frac{\dot{W}_{net,ORC} + \dot{E}x_{heating} + \dot{E}x_{cooling} + \dot{E}x_{H_2} + \dot{E}x_{36} + \dot{E}x_{41}}{\dot{E}x_{biomass}} \tag{6.11}$$

Table 6.2 Expressions for exergy destruction rates for components of system II

Component	Exergy destruction rate expression
Combustor	$\dot{E}x_{D,Comb} = \dot{E}x_{29} + \dot{E}x_{30} - \dot{E}x_{31}$
ORC evaporator	$\dot{E}x_{D,Evp} = \dot{E}x_{32} + \dot{E}x_{26} - \dot{E}x_{27} - \dot{E}x_{33}$
ORC turbine	$\dot{E}x_{D,T} = \dot{E}x_{27} - \dot{W}_T - \dot{E}x_{28}$
Heating process	$\dot{E}x_{D,heat} = \dot{E}x_{28} - \dot{E}x_Q - \dot{E}x_{24}$
ORC pump	$\dot{E}x_{D,P} = \dot{E}x_{25} + \dot{W}_P - \dot{E}x_{26}$
Absorption condenser	$\dot{E}x_{D,Cond} = \dot{E}x_{19} + \dot{E}x_{20} - \dot{E}x_8 - \dot{E}x_{21} + \dot{E}x_7$
Expansion valves	$\dot{E}x_{D,Exv} = \dot{E}x_{18} - \dot{E}x_{19} + \dot{E}x_8 - \dot{E}x_9 + \dot{E}x_{15} - \dot{E}x_{16} + \dot{E}x_5 - \dot{E}x_6$
Absorption evaporator	$\dot{E}x_{D,Evp} = \dot{E}x_9 + \dot{E}x_{21} - \dot{E}x_{23} - \dot{E}x_{10}$
Absorber	$\dot{E}x_{D,Abs} = \dot{E}x_{10} + \dot{E}x_6 + \dot{E}x_{38} - \dot{E}x_1 - \dot{E}x_{39}$
Absorption pump	$\dot{E}x_{D,P} = \dot{E}x_1 + \dot{W}_P - \dot{E}x_2$
Absorption heat exchanger I	$\dot{E}x_{D,HExI} = \dot{E}x_2 + \dot{E}x_4 - \dot{E}x_3 - \dot{E}x_5$
Absorption heat exchanger h	$\dot{E}x_{D,HExh} = \dot{E}x_3 + \dot{E}x_{14} - \dot{E}x_{13} - \dot{E}x_{15}$
High temperature absorption generator	$\dot{E}x_{D,Genh} = \dot{E}x_{24} + \dot{E}x_{13} - \dot{E}x_{14} - \dot{E}x_{17} - \dot{E}x_{25}$
Low temperature absorption generator	$\dot{E}x_{D,GenL} = \dot{E}x_{17} - \dot{E}x_{18} - \dot{E}x_Q$
PEM electrolyzer	$\dot{E}x_{D,PEM} = \dot{E}x_{22} + \dot{W}_{PEM} - \dot{E}x_{24} - \dot{E}x_{23}$
Domestic hot water heater	$\dot{E}x_{D,DWH} = \dot{E}x_{33} + \dot{E}x_{35} - \dot{E}x_{36} - \dot{E}x_{34}$
RO pump	$\dot{E}x_{D,ROPump} = \dot{E}x_{39} + \dot{W}_P - \dot{E}x_{40}$
RO desalination unit	$\dot{E}x_{D,ROdesalination} = \dot{E}x_{40} - \dot{E}x_{41} - \dot{E}x_{42}$
RO hydraulic turbine	$\dot{E}x_{D,hturbine} = \dot{E}x_{42} - \dot{W}_T - \dot{E}x_{43}$

where

$$\dot{E}x_{heating} = \dot{Q}_{cond}\left(1 - \frac{T_0}{T_{cond}}\right) \tag{6.12}$$

$$\dot{E}x_{cooling} = \dot{Q}_{cooling}\left(\frac{T_0 - T_{EVP}}{T_{EVP}}\right) \tag{6.13}$$

$$\dot{E}x_{H_2} = \dot{m}_{H_2} ex_{H_2} \tag{6.14}$$

$$\dot{E}x_{35} = \dot{m}_{35}(h_{35} - h_0) - T_0(s_{35} - s_0) \tag{6.15}$$

Also, $\dot{E}x_{biomass}$ is the exergy of biomass, defined as [24]:

$$\dot{E}x_{biomass} = \dot{m}_{biomass}\beta LHV_{mois} \tag{6.16}$$

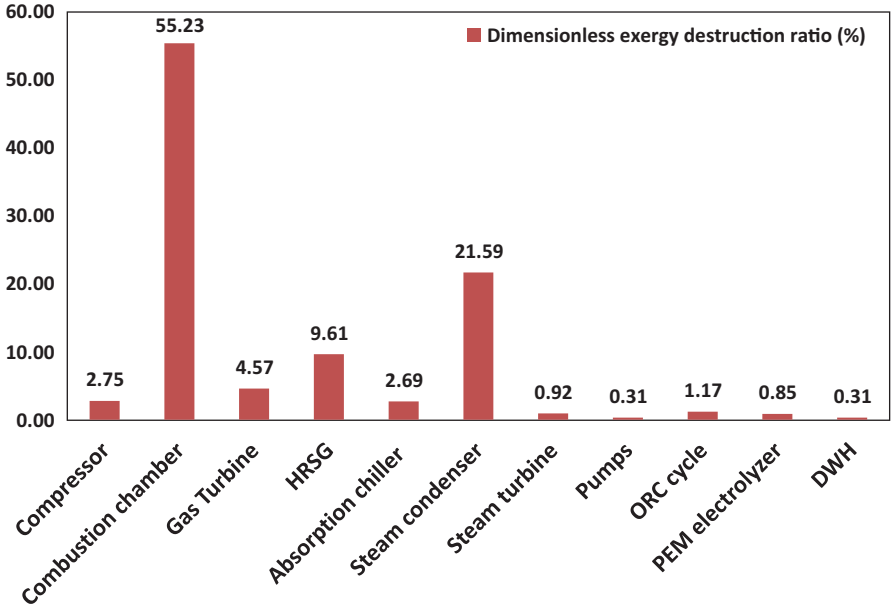

Fig. 6.10 Dimensionless exergy destruction ratio for the multigeneration system I and its components

Here, β is defined as

$$\beta = \frac{1.0414 + 0.0177\left(\frac{\mathrm{H}}{\mathrm{C}}\right) - 0.3328\left(\frac{\mathrm{O}}{\mathrm{C}}\right)\left\{1 + 0.0537\left(\frac{\mathrm{H}}{\mathrm{C}}\right)\right\}}{1 - 0.4021\left(\frac{\mathrm{O}}{\mathrm{C}}\right)} \tag{6.17}$$

Exergy Analysis of System III

The exergy destructions for all components in multigeneration system III (Fig. 6.10) are shown in Table 6.3.The exergy efficiency is defined as the product exergy output divided by the exergy input. According to Yamada et al. [88], the exergy efficiency of the ORC power generation cycle in an OTEC system is given as

$$\psi_{Power} = \frac{\dot{W}_{net}}{\dot{E}x_m} = \frac{\dot{W}_{net,OTEC}}{\dot{E}x_{in,WS} + \dot{E}x_{in,CS}} \tag{6.18}$$

$$\psi_{CHP} = \frac{\dot{W}_{net,OTEC} + \dot{W}_{PV/T}}{\dot{E}x_{in,WS} + \dot{E}x_{in,CS} + \dot{E}x_{Sun}} \tag{6.19}$$

Table 6.3 Expressions for exergy destruction rates for components of system III

Component	Exergy destruction rate expression
Warm sea water pump	$\dot{E}x_{D,P} = \dot{E}x_1 + \dot{W}_P - \dot{E}x_2$
Cold sea water pump	$\dot{E}x_{D,P} = \dot{E}x_9 + \dot{W}_P - \dot{E}x_{10}$
Solar collector	$\dot{E}x_{D,collector} = \dot{E}x_2 + \dot{E}x_{sun} - \dot{E}x_3$
Turbine	$\dot{E}x_{D,T} = \dot{E}x_5 - \dot{W}_T - \dot{E}x_6$
Condenser	$\dot{E}x_{D,Cond} = \dot{E}x_6 + \dot{E}x_{10} - \dot{E}x_7 - \dot{E}x_{11}$
WF pump	$\dot{E}x_{D,P} = \dot{E}x_7 + \dot{W}_P - \dot{E}x_8$
Solar PV/T	$\dot{E}x_{D,collector} = \dot{E}x_{41} + \dot{E}x_{sun} - \dot{E}x_{40}$
Absorption condenser	$\dot{E}x_{D,Cond} = \dot{E}x_{39} - \dot{E}x_{26} - \dot{E}x_Q$
Absorption expansion valves	$\dot{E}x_{D,EXV} = \dot{E}x_{26} + \dot{E}x_{37} - \dot{E}x_{27} - \dot{E}x_{38}$
Absorption evaporator	$\dot{E}x_{D,EVP} = \dot{E}x_{27} - \dot{E}x_{29} + \dot{E}x_Q$
Absorber	$\dot{E}x_{D,Abs} = \dot{E}x_{28} + \dot{E}x_{38} + \dot{E}x_{31} - \dot{E}x_{32} - \dot{E}x_{33}$
Absorption pump	$\dot{E}x_{D,P} = \dot{E}x_{33} + \dot{W}_P - \dot{E}x_{34}$
Absorption heat exchanger	$\dot{E}x_{D,HEX} = \dot{E}x_{34} + \dot{E}x_{36} - \dot{E}x_{35} - \dot{E}x_{37}$
Absorption generator	$\dot{E}x_{D,Gen} = \dot{E}x_{35} + \dot{E}x_{40} - \dot{E}x_{41} - \dot{E}x_{33} - \dot{E}x_{36}$
PEM electrolyzer	$\dot{E}x_{D,PEM} = \dot{E}x_{29} + \dot{W}_{PEM} - \dot{E}x_{22} - \dot{E}x_{21}$
RO pump	$\dot{E}x_{D,RO\ Pump} = \dot{E}x_{13} + \dot{W}_P - \dot{E}x_{14}$
RO desalination unit	$\dot{E}x_{D,RO\ desalination} = \dot{E}x_{14} - \dot{E}x_{10} - \dot{E}x_{15}$
RO hydraulic turbine	$\dot{E}x_{D,h\ turbine} = \dot{E}x_{16} - \dot{W}_T - \dot{E}x_{17}$

$$\psi_{multi} = \frac{\dot{W}_{net,ORC} + \dot{W}_{PV/T} + \dot{E}x_{cooling} + \dot{E}x_{H_2} + \dot{E}x_{22}}{\dot{E}x_{in,WS} + \dot{E}x_{in,CS} + \dot{E}x_{Sun}} \tag{6.20}$$

where

$$\dot{E}x_{in,WS} = \dot{m}_{in,WS}\left[(h_{WS,in} - h_0) - T_0(s_{WS,in} - s_0)\right] \tag{6.21}$$

$$\dot{E}x_{in,CS} = \dot{m}_{in,CS}\left[(h_{CS,in} - h_0) - T_0(s_{CS,in} - s_0)\right] \tag{6.22}$$

Here, the reference-environment state is taken to be $P_0 = 1.01$ bar and $T_0 = 298.15$ K.

6.5 Results and Discussion

In order to enhance the understanding of the system's performance, it is important to use several analyses to see how this performance varies with design parameters. In this section, the results of thermodynamic modeling, exergy, economic and environmental impact assessment, and optimization are explained. Exergy analysis can help develop strategies and guidelines for more efficient and effective use of energy, and is utilized to study various thermal processes, especially power generation, CHP, trigeneration and multigeneration. The exergy analysis includes the determination of the exergy destruction rate and exergy efficiency of each component in the system and also determines the overall exergy efficiency of the multigeneration system. Exergy analysis also helps to identify and quantify the source of irreversibilities in the systems that are associated with each component. Economic analysis shows the total cost rate of the system, cost of each component, cost of electricity and cost of environmental impacts.

Exergy Analysis of System I

The exergy analysis results are summarized in Fig. 6.9, and show that the highest exergy destruction occurs in the combustion chamber (CC), mainly due to the irreversibilities associated with combustion and the large temperature difference between the air entering the CC and the flame temperature. The condenser in the Rankine cycle exhibits the next largest exergy destruction, mainly due to the temperature difference between two fluid streams passing through it, but also due to the pressure drop across the device.

Figure 6.10 shows for each component the dimensionless exergy destruction ratio. This measure is useful for prioritizing exergy losses in an intuitive manner. Both exergy destruction and the dimensionless exergy destruction ratio are higher in the combustor than in other components, suggesting that it would likely be worthwhile to focus improvement efforts on this component. Moreover, the results show that the absorption cycle does not exhibit significant exergy destructions, in part because it does not directly utilize fuel energy but instead uses steam produced by the HRSG.

In order to better understand the system performance, energy and exergy efficiency of each subsystem are calculated (see Fig. 6.10). It is seen that energy and exergy efficiencies are higher for the multigeneration system compared to other cycles when it is not configured in an integrated manner. It is also seen that both energy and exergy efficiencies for the multigeneration system are almost double those of a power generation system, mainly due to an increase in the numerator of exergy efficiency.

Table 6.4 Parameter values from modeling and energy and exergy analyses of the system II

Parameter	Unit	Value
Biomass flow rate, $\dot{m}_f$	kg/s	0.30
Heating load, $\dot{Q}_{Heating}$	kW	2383
Cooling load, $\dot{Q}_{Cooling}$	kW	2560
Net output power, $\dot{W}_{Net}$	kW	500.47
Exergy efficiency, ψ	%	28.82
Absorption chiller COP	–	1.63
ORC mass flow rate, $\dot{m}_{ORC}$	kg/s	4.84
Hydrogen production mass flow rate, $\dot{m}_{H_2}$	kg/day	2
Hot water mass flow rate, $\dot{m}_{HW}$	kg/s	0.78
Fresh water mass flow rate, $\dot{m}_{fresh}$	Kg/s	1.93
Specific CO_2 emission, ε	kg/MWh	358
Total cost rate	$/h	476
Cost of environmental impact	$/h	48.47
Total exergy destruction rate	kW	5393
Power to cooling ratio	–	0.19
Power to heating ratio	–	0.20

Exergy Analysis of Case Study II

Table 6.4 lists the thermodynamic specifications of the multigeneration system, including heating and cooling loads, the electricity generated by the turbines, the COP of the absorption chiller, and the mass flow rates of biomass, hydrogen and hot water. The analysis described earlier is used to evaluate output parameters including exergy efficiency and exergy destruction rate of the components in the system considered, as well as the carbon dioxide emissions in kg/MWh. These parameters are examined while varying the ORC evaporator pinch point temperature, the ORC pump inlet temperature, the turbine inlet pressure and the biomass mass flow rate. The exergy efficiency and CO_2 emissions are calculated for three cases: electrical power, cogeneration and multigeneration. The exergy analysis results are summarized in Fig. 6.12, and show that the highest exergy destruction occurs in the combustor, mainly due to the irreversibilities associated with combustion and the large temperature difference between the air entering the combustor and the flame temperature. The double-effect absorption chiller heat exhibits the next largest exergy destruction, mainly due to the temperature difference between two fluid streams passing through all heat exchangers as the pressure drop across the device.

Table 6.5 Input data for the system simulation of OTEC system

Parameter	Value	Parameter	Value
Turbine isentropic efficiency, η_T	0.80	Warm seawater mass flow rate (kg/s)	150
Generator mechanical efficiency, η_G	0.90	Cold sea water mass flow rate (kg/s)	150
Working fluid pump isentropic efficiency, η_{WFP}	0.78	Cold sea water pipe length (m)	1000
Seawater pumps isentropic efficiency, η_P	0.80	Cold seawater pipe inner diameter (m)	0.70
Ambient temperature (°C)	25	Warm sea water pipe length (m)	50
Solar radiation incident on collector surface, I (W/m^2)	700	Warm sea water pipe length (m)	0.70
Warm sea water temperature, T_{WSI} (°C)	22	Solar collector effective area (m^2)	5000
Cold sea water temperature at depth of 1000 m, T_{CSI} (°C)	4	Electrolyzer working temperature (°C)	80
PV/T solar collector length (m)	1.2	PV/T solar collector width (m)	0.54
Absorption chiller evaporator temperature (°C)	5	OTEC evaporator pinch point temperature (°C)	3
Sea water salinity (ppm)	36000	PV/T air mass flow rate (kg/s)	2

Exergy Analysis Results for Case Study III

In order to conduct the simulation, input data are required. For each subsystem certain reliable data are inputted to the simulation code in order to determine the outputs. Table 6.5 lists the input parameters for the OTEC system simulation. In addition, Table 6.6 lists the parameter used to simulate the PEM electrolyzer. Table 6.7 lists the thermodynamic specifications of the multigeneration system, including cooling load, the electricity generated by the turbines, the COP of the absorption chiller, and the mass flow rates of biomass, hydrogen, hot water and fresh water production.

The exergy analysis results are summarized in Fig. 6.13, and show that the highest exergy destruction occurs in the solar collectors, mainly due to the irreversibilities associated with the high temperature of sun which creates high exergy input. Moreover, the temperature difference between the solar cell and inlet air temperature results in a significant entropy generation. The OTEC Rankine cycle exhibits the next largest exergy destruction, mainly due to the temperature difference between two fluid streams passing through the components, along with the pressure drop across the device Fig. 6.11.

Table 6.6 Input parameters used to model PEM electrolysis

Parameter	Value
P_{o_2} (atm)	1.0
P_{H_2} (atm)	1.0
T_{PEM} (°C)	80
$E_{\text{act,a}}$ (kJ/mol)	76
$E_{\text{act,c}}$ (kJ/mol)	18
λ_{a}	14
λ_{c}	10
D (μm)	100
J_a^{ref} (A/m^2)	1.7×10^5
J_c^{ref} (A/m^2)	4.6×10^3
F (C/mol)	96,486

Table 6.7 Parameter values resulting from energy and exergy analyses of the system III

Parameter	Value
Net power output, $\dot{W}_{net}$ (kW)	72.49
Exergy efficiency, Ψ (%)	0.37
Sustainability Index, *SI*	1.29
Total exergy destruction rate, $\dot{E}x_{D,tot}$ (kW)	1351
Hydrogen production rate, $\dot{m}_{H_2}$ (kg/hr)	0.26
Cooling load (kW)	105
Fresh water mass flow rate (kg/s)	0.23
Total cost rate ($/h)	176.35
PEM electrolyzer exergy efficiency, Ψ_{PEM} (%)	56.32
Warm surface pump power, $\dot{W}_{WS}$ (kW)	1.39
Cold surface pump power, $\dot{W}_{CS}$ (kW)	3.34
Working fluid pump power, $\dot{W}_{WF}(kW)$	1.12

Figure 6.13 shows the dimensionless exergy destruction ratio for each component. This measure is useful for prioritizing exergy losses in an intuitive manner. Both exergy destruction and the dimensionless exergy destruction ratio are higher in solar collectors than in any other component, suggesting that it would likely be worthwhile to focus improvement efforts on this component. Moreover, the results show that, the absorption cycle and RO desalination unit do not exhibit significant exergy destructions, since it does not directly utilize fuel energy but uses heat produced by the PV/T and work instead.

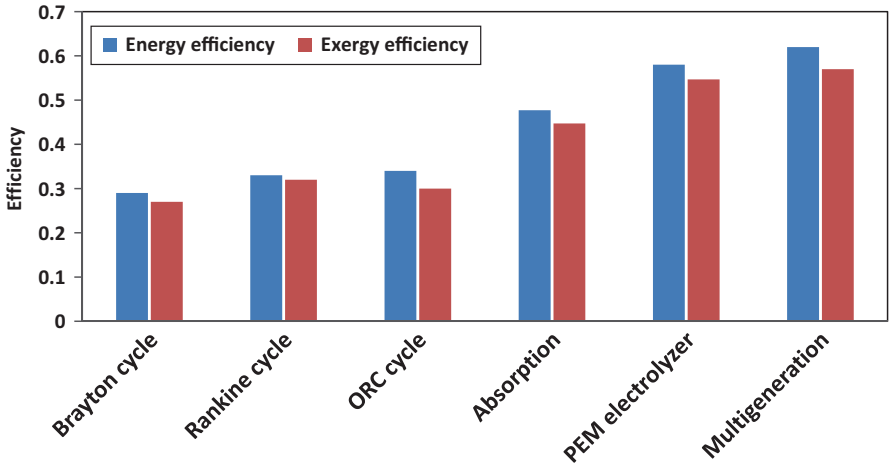

Fig. 6.11 Energy and exergy efficiency for the subsystems of the multigeneration system I

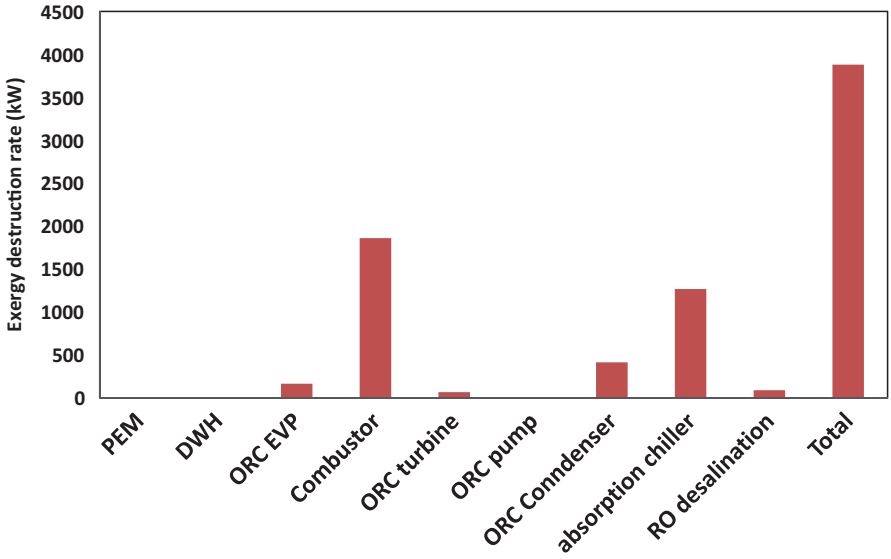

Fig. 6.12 Exergy destruction rates for the multigeneration system II and its components

6.6 Comparison and generalization

In this section, the comprehensive thermodynamic modelling, exergy analyses, environmental impact assessments, and multi-objective optimization of three newly proposed multigeneration systems for heating, cooling, electricity generation,

Table 6.8 Comparison of three novel multigeneration systems

Parameter	$\dot{W}_{net}$ (kW)	$\dot{Q}_{heat}$ (kW)	$\dot{Q}_{cooling}$ (kW)	H_2 (kg/h)	$\dot{m}_{DWH}$ (kg/s)	$\dot{m}_{FW}$ (kg/s)	$\dot{Z}_{tot}$ ($/h)	Ψ	CO_2 (kg/kWh)
System I	11038	5788	1262	1.25	3.58	NA	1090	0.60	132
System II	500	2383	2560	0.08	0.8	1.9	476	0.3	0.36
System III	73	NA	105	0.2	NA	0.2	152	0.37	0

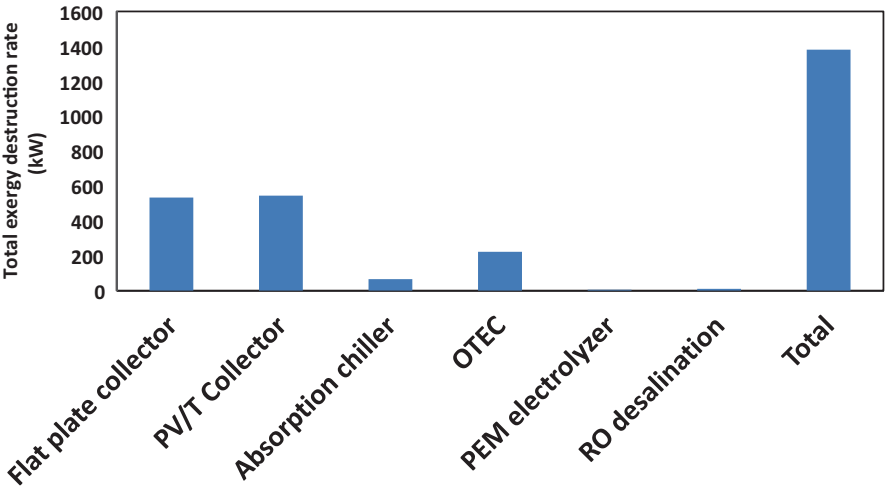

Fig. 6.13 Exergy destruction rates for the Integrated OTEC based multigeneration system and its components

hydrogen, hot water and fresh water productions are reported for insights they provide. Since these three systems have different prime movers, the comparison needs different criteria. Table 6.8 lists the useful outputs of each multigeneration energy system. This data shows that although the net power output of system I is much higher than that of alternative systems, the CO_2 emissions and total cost rate are higher compared to other systems fig. 6.14.

Since the capacity of each system is different, it is difficult to meaningfully compare them. One approach is to normalize each system and then compare them. In order to normalize the cost, the total cost rate of each system is divided by the energy of useful outputs and the final cost per kWh of products is compared. The following equations are used to normalize the cost:

$$C_{System} = \frac{\dot{Z}_{tot,I}}{\sum \dot{W}_{net} + \sum \dot{Q}_{heat} + \sum \dot{Q}_{cooling} + \dot{E}n_{H_2} + \dot{E}n_{DWH} + \dot{E}n_{FW}} \tag{6.23}$$

Here,

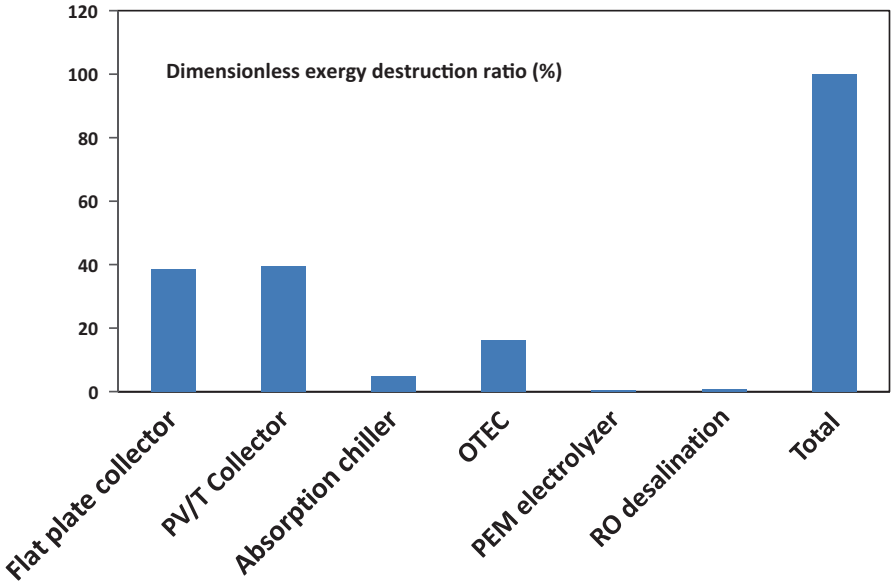

Fig. 6.14 Dimensionless exergy destruction ratio for the multigeneration system III and its components

Table 6.9 Comparison of normalized cost for each multigeneration system

Name of system	Normalized cost ($/kWh)
System I (Gas turbine based)	0.06
System II (Biomass based)	0.08
System III (OTEC based)	0.71

En_{H_2} is the energy of hydrogen production, En_{DWH} is the energy of hot water at 60 °C and En_{FW} is the energy of fresh water production. Table 6.9 lists the normalized cost for each multigeneration system. The results show that the normalized cost of the gas turbine multigeneration energy system is less those other systems; however, the CO_2 emissions are relatively high. By contrast, the normalized cost of the integrated OTEC multigeneration system is higher than the other two, but does not have any CO_2 emissions at all. In conclusion, the comparison between multigeneration systems strongly depends on the stated priorities of the designers and engineers. For example, if the priority is to have a system without any emissions and the location is close to the sea, the OTEC system is the best choice. If the plant is going to be installed in a rural area with sufficient biomass, the second multigeneration system is preferred. In addition, the amount of each useful output can help designers to decide which system they should select. For instance, the gas turbine multigeneration system can provide 10 MW of electricity, while OTEC system can only provide 100 kW of electricity.

In summary, the comparison of systems indicates that there are several criteria to be considered before undertaking the design of a multigeneration energy system:

- Location of the plant.
- Electricity, heating and cooling requirements of the system.
- Budget for the system.
- Environmental concerns and global warming mitigation.
- Availability and cost of fuel for each system component.

Concluding Remarks

The comprehensive thermodynamic modeling and exergy analyses of newly proposed integrated energy systems for heating, cooling, electricity generation, hydrogen and hot water production have provided useful insights. Three different integrated multigeneration systems depending on location, energy resource availability and cost are selected and analyzed. This chapter provides several interesting results on using multigeneration energy systems to increase the overall efficiency of the plant and to provide the needs. These outcomes of this chapter can assist designers in developing more energy efficient systems in an integration fashion. Integrated energy systems have the potential to reduce environmental impacts of the systems and mitigate the global warming which eventually results in the better sustainability. Micro-gas turbine integrated system results show that the combustion chamber, steam condenser and HRSG are the main sources of irreversibility, with the high exergy destruction attributable to the high temperature difference for heat transfer in both devices and the reaction in the combustion chamber. In addition, the multigeneration cycle exhibits less CO_2 and CO emissions than micro gas turbine and CHP cycles.

The results of biomass based integrated system show that the combustor and ORC evaporator are the two main sources of irreversibility, with the highest exergy destruction rate due to the high temperature difference of heat transfer in both devices and the reaction in the combustor. System performance is notably affected by pinch point temperature, ORC turbine inlet pressure, and ORC pump inlet temperature. The results of ocean thermal energy conversion integrated energy systems show that system performance is notably affected by warm surface mass flow rate, solar radiation intensity, condenser temperature, PV/T collector length, PV/T collector width, PV/T inlet air mass flow rate and evaporator pinch point temperature difference (*PP*). Both exergy destruction and the dimensionless exergy destruction ratio are higher in solar collectors than in other components, suggesting that it would be worthwhile to focus efforts on improving this component.

Nomenclature

c_p	specific heat at constant pressure, kJ/kg°C
ex	specific exergy, kJ/kg
$\dot{E}x_D$	exergy destruction rate, kW

J	current density, A/m^2
J_o	exchange current density, A/m^2
J_i^{ref}	pre-exponential factor, A/m^2
L	length, m
h	specific enthalpy, kJ/kg
$\dot{m}$	mass flow rate, kg/s
$\dot{N}$	molar mass flow rate, mol/s
T	temperature (°C)
P	pressure, kPa
$\dot{Q}$	heat transfer rate, kW
R	gas constant, kJ/kg K
R_{PEM}	proton exchange membrane resistance, Ω
s	specific entropy, kJ/kg K
V	voltage potential, V
V_0	reversible potential, V
V_{act}	activation overpotential, V
$V_{act,a}$	anode activation overpotential, V
$V_{act,c}$	cathode activation overpotential, V
$\dot{W}$	work rate (kW)

Greek Letters

η	energy efficiency
λ_a	water content at the anode-membrane interface, Ω^{-1}
λ_c	water content at the cathode-membrane interface, Ω^{-1}
$\lambda(x)$	water content at location x in the membrane, Ω^{-1}
σ_{PEM}	proton conductivity in PEM (s/m)
$\sigma(x)$	local ionic PEM conductivity (s/m)
Ψ	exergy efficiency
ω	entertainment ratio

Subscripts

a	anode
c	cathode
CHP	combined heat and power
D	destruction
EXV	expansion valve
HRVG	heat recover vapor generator
HW	hot water
Multi	multigeneration
ORC	organic Rankine cycle
PRH	preheater
tot	total
WF	working fluid
Cond	Condenser

Superscripts

. rate

References

1. Dincer I (2000) Renewable energy and sustainable development: a crucial review. Renew Sustain Energy Rev 4:157–175
2. Ozgur Colpan C, Dincer I, Hamdullahpur F (2009) The reduction of greenhouse gas emissions using various thermal systems in a landfill site. Int J Global Warming 1:89–105
3. Spahni R, Chappellaz J, Stocker TF, Loulergue L, Hausammann G, Kawamura K, Flückiger J, Schwander J, Raynaud D, Masson-Delmotte V (2005) Atmospheric methane and nitrous oxide of the late Pleistocene from Antarctic ice cores Science 310:1317–1321
4. Ahmadi P, Dincer I (2010) Exergoenvironmental analysis and optimization of a cogeneration plant system using Multimodal Genetic Algorithm (MGA). Energy 35:5161–5172
5. Ahmadi P (2013) Modeling, analyses and optimization of integrated energy systems for multigeneration purposes Ph.D Disertation. University of Ontario Institute of Technology, Canada
6. Ahmadi P, Rosen MA, Dincer I (2011) Greenhouse gas emission and exergo-environmental analyses of a trigeneration energy system. Int J Greenh Gas Control 5:1540–1549
7. Dincer I, Zamfirescu C (2012) Renewable-energy-based multigeneration systems. Int J Energy Res 36:1403–1415
8. Ahmadi P, Rosen MA, Dincer I (2012) Multi-objective exergy-based optimization of a polygeneration energy system using an evolutionary algorithm. Energy 46:21–31
9. Khaliq A, Kumar R, Dincer I (2009) Performance analysis of an industrial waste heat-based trigeneration system. Int J Energy Res 33:737–744
10. Ratlamwala T, Dincer I, Gadalla M (2012) Energy and exergy analyses of an integrated solar-based desalination quadruple effect absorption system for freshwater and cooling production. Int J Energy Res 37:1569–1579
11. Horlock JH (2003) Advanced gas turbine cycles. Pergamon Press Oxford, UK.
12. Haseli Y, Dincer I, Naterer G (2008) Thermodynamic modeling of a gas turbine cycle combined with a solid oxide fuel cell. Int J Hydrog Energy 33:5811–5822
13. Srinivas N, Deb K (1994) Muiltiobjective optimization using nondominated sorting in genetic algorithms. Evolut Comput 2:221–248
14. Huangfu Y, Wu J, Wang R, Xia Z (2007) Experimental investigation of adsorption chiller for micro-scale BCHP system application. Energy Build 39:120–127
15. Mago PJ, Hueffed A, Chamra LM (2010) Analysis and optimization of the use of CHP–ORC systems for small commercial buildings. Energy Build 42:1491–1498
16. Mago PJ, Smith AD (2012) Evaluation of the potential emissions reductions from the use of CHP systems in different commercial buildings. Build Environ 53:74–82
17. Mago PJ, Hueffed AK (2010) Evaluation of a turbine driven CCHP system for large office buildings under different operating strategies. Energy Build 42:1628–1636
18. Bianchi M, De Pascale A, Melino F (2013) Performance analysis of an integrated CHP system with thermal and electric energy storage for residential application. Appl Energy
19. Havelský V (1999) Energetic efficiency of cogeneration systems for combined heat, cold and power production. Int J Refrig 22:479–485
20. Mıguez J, Murillo S, Porteiro J, Lopez L (2004) Feasibility of a new domestic CHP trigeneration with heat pump: I. Design and development. Appl Therm Eng 24:1409–1419
21. Porteiro J, Mıguez J, Murillo S, Lopez L (2004) Feasibility of a new domestic CHP trigeneration with heat pump: II. Availability analysis. Appl Therm Eng 24:1421–1429

22. Cihan A, Hacıhafızoglu O, Kahveci K (2006) Energy–exergy analysis and modernization suggestions for a combined-cycle power plant. Int J Energy Res 30:115–126
23. Barelli L, Bidini G, Gallorini F, Ottaviano A (2011) An energetic–exergetic analysis of a residential CHP system based on PEM fuel cell. Appl Energy 88:4334–4342
24. Bingöl E, Kılkış B, Eralp C (2011) Exergy based performance analysis of high efficiency poly-generation systems for sustainable building applications. Energy Build 43:3074–3081
25. El-Emam RS, Dincer I (2011) Energy and exergy analyses of a combined molten carbonate fuel cell–Gas turbine system. Int J Hydrog Energy 36:8927–8935
26. Akkaya AV, Sahin B, Huseyin Erdem H (2008) An analysis of SOFC/GT CHP system based on exergetic performance criteria. Int J Hydrog Energy 33:2566–2577
27. Al-Sulaiman FA, Dincer I, Hamdullahpur F (2010) Energy analysis of a trigeneration plant based on solid oxide fuel cell and organic Rankine cycle. Int J Hydrog Energy 35:5104–5113
28. Rosen MA, Dincer I (2003) Exergoeconomic analysis of power plants operating on various fuels. Appl Therm Eng 23:643–658
29. Ameri M, Ahmadi P, Hamidi A: Energy, exergy and exergoeconomic analysis of a steam power plant (2009) A case study. Int J Energy Res 33:499–512
30. Balli O, Aras H, Hepbasli A (2007) Exergetic performance evaluation of a combined heat and power (CHP) system in Turkey. Int J Energy Res 31:849–866
31. Balli O, Aras H, Hepbasli A (2008) Exergoeconomic analysis of a combined heat and power (CHP) system. Int J Energy Res 32:273–289
32. Kwak HY, Byun GT, Kwon YH, Yang H (2004) Cost structure of CGAM cogeneration system. Int J Energy Res 28:1145–1158
33. Pospisil J, Fiedler J, Skala Z, Baksa M (2006) Comparison of cogeneration and trigeneration technology for energy supply of tertiary buildings. WSEAS Trans Heat Mass Transf 1:262–267
34. Al-Sulaiman FA, Hamdullahpur F, Dincer I (2011) Performance comparison of three trigeneration systems using organic rankine cycles. Energy 36:5741–5754
35. Martins L, Fábrega F, d'Angelo J (2012) Thermodynamic performance investigation of a trigeneration cycle considering the influence of operational variables. Procedia Eng 42:2061–2070
36. Calva ET, Núnez MP, Toral M (2005) Thermal integration of trigeneration systems. Appl Therm Eng 25:973–984
37. Huang Y, Wang Y, Rezvani S, McIlveen-Wright D, Anderson M, Hewitt N (2011) Biomass fuelled trigeneration system in selected buildings. Energy Convers Manage Â52:2448–2454
38. Rocha M, Andreos R, Simões-Moreira J (2012) Performance tests of two small trigeneration pilot plants. Appl Therm Eng Â41:84–91
39. Huicochea A, Rivera W, Gutiérrez-Urueta G, Bruno JC, Coronas A (2011) Thermodynamic analysis of a trigeneration system consisting of a micro gas turbine and a double effect absorption chiller. Appl Therm Eng 31:3347–3353
40. Chicco G, Mancarella P (2005) Planning aspects and performance indicators for small-scale trigeneration plants. In Future Power Systems, 2005 International Conference on p 6
41. Chicco G, Mancarella P (2006) Planning evaluation and economic assessment of the electricity production from small-scale trigeneration plants. WSEAS Trans Power Syst 1:393–400
42. Aghahosseini S, Dincer I, Naterer G (2011) Integrated gasification and Cu–Cl cycle for trigeneration of hydrogen, steam and electricity. Int J Hydrog Energy 36:2845–2854
43. Minciuc E, Le Corre O, Athanasovici V, Tazerout M, Bitir I (2003) Thermodynamic analysis of tri-generation with absorption chilling machine. Appl Therm Eng 23:1391–1405
44. Moya M, Bruno J, Eguia P, Torres E, Zamora I, Coronas A (2011) Performance analysis of a trigeneration system based on a micro gas turbine and an air-cooled, indirect fired, ammonia–water absorption chiller. Appl Energy 88:4424–4440
45. Velumani S, Enrique Guzmán C, Peniche R, Vega R (2010) Proposal of a hybrid CHP system: SOFC/microturbine/absorption chiller. Int J Energy Res 34:1088–1095
46. Buck R, Friedmann S (2007) Solar-assisted small solar tower trigeneration systems. Transactions-american society of mechanical engineers. J Sol Energy Eng 129:349

47. Dincer I, Rosen MA (2012) Exergy: energy, environment and sustainable development. 2nd Edition, Elsevier Science
48. Santo D (2012) Energy and exergy efficiency of a building internal combustion engine trigeneration system under two different operational strategies. Energy Build 53:28–38
49. Ebrahimi M, Keshavarz A, Jamali A (2012) Energy and exergy analyses of a micro-steam CCHP cycle for a residential building. Energy Build 45:202–210
50. Khaliq A (2009) Exergy analysis of gas turbine trigeneration system for combined production of power heat and refrigeration. Int J Refrig 32:534–545
51. Kong X, Wang R, Huang X (2004) Energy efficiency and economic feasibility of CCHP driven by stirling engine. Energy Convers Manage 45:1433–1442
52. Ziher D, Poredos A (2006) Economics of a trigeneration system in a hospital. Appl Therm Eng 26:680–687
53. Temir G, Bilge D (2004) Thermoeconomic analysis of a trigeneration system. Appl Therm Eng 24:2689–2699
54. Ehyaei M, Mozafari A (2010) Energy, economic and environmental (3E) analysis of a micro gas turbine employed for on-site combined heat and power production. Energy Build 42:259–264
55. Ozgener O, Hepbasli A (2005) Exergoeconomic analysis of a solar assisted ground-source heat pump greenhouse heating system. Appl Therm Eng 25:1459–1471
56. Ozgener O, Hepbasli A, Ozgener L (2007) A parametric study on the exergoeconomic assessment of a vertical ground-coupled (geothermal) heat pump system. Build Environ 42:1503–1509
57. Dincer I (2007) Environmental and sustainability aspects of hydrogen and fuel cell systems. Int J Energy Res 31:29–55
58. Amrollahi Z, Ertesvåg IS, Bolland O (2011) Thermodynamic analysis on post-combustion CO capture of natural-gas-fired power plant. Int J Greenh Gas Control 5:422–426
59. Petrakopoulou F, Boyano A, Cabrera M, Tsatsaronis G (2011) Exergoeconomic and exergoenvironmental analyses of a combined cycle power plant with chemical looping technology. Int J Greenh Gas Control 5:475–482
60. Sahoo P (2008) Exergoeconomic analysis and optimization of a cogeneration system using evolutionary programming. Appl Therm Eng 28:1580–1588
61. Sayyaadi H, Sabzaligol T (2009) Exergoeconomic optimization of a 1000 MW light water reactor power generation system. Int J Energy Res 33:378–395
62. Haseli Y, Dincer I, Naterer G (2008) Optimum temperatures in a shell and tube condenser with respect to exergy. Int J Heat Mass Transf 51:2462–2470
63. Sayyaadi H, Nejatolahi M (2011) Multi-objective optimization of a cooling tower assisted vapor compression refrigeration system. Int J Refrig 34:243–256
64. Ahmadi P, Dincer I, Rosen MA (2011) Exergy, exergoeconomic and environmental analyses and evolutionary algorithm based multi-objective optimization of combined cycle power plants. Energy 36:5886–5898
65. Sayyaadi H, Babaelahi M (2011) Multi-objective optimization of a joule cycle for re-liquefaction of the liquefied natural gas. Appl Energy 88:3012–3021
66. Ghaebi H, Saidi M, Ahmadi P (2012) Exergoeconomic optimization of a trigeneration system for heating, cooling and power production purpose based on TRR method and using evolutionary algorithm. Appl Therm Eng 36:113–125
67. Kavvadias K, Maroulis Z (2010) Multi-objective optimization of a trigeneration plant. Energy Policy 38:945–954
68. Al-Sulaiman FA, Dincer I, Hamdullahpur F (2013) Thermoeconomic optimization of three trigeneration systems using organic Rankine cycles: Part I–Formulations. Energy Convers Manage 59:199–208
69. Wang J, Yan Z, Wang M, Li M, Dai Y (2013) Multi-objective optimization of an organic Rankine cycle (ORC) for low grade waste heat recovery using evolutionary algorithm. Energy Convers Manage 71:146–158

70. Shirazi A, Aminyavari M, Najafi B, Rinaldi F, Razaghi M (2012) Thermal–economic–environmental analysis and multi-objective optimization of an internal-reforming solid oxide fuel cell–gas turbine hybrid system. Int J Hydrog Energy
71. Hosseini M, Dincer I, Ahmadi P, Avval HB, Ziaasharhagh M (2011) Thermodynamic modelling of an integrated solid oxide fuel cell and micro gas turbine system for desalination purposes. Int J Energy Res 37:426–434
72. Ratlamwala T, Gadalla M, Dincer I (2011) Performance assessment of an integrated PV/T and triple effect cooling system for hydrogen and cooling production. Int J Hydrog Energy 36:11282–11291
73. Ratlamwala T, Dincer I, Gadalla M (2012) Performance analysis of a novel integrated geothermal-based system for multi-generation applications. Appl Therm Eng 40:71–79
74. Ozturk M, Dincer I (2012) Thermodynamic analysis of a solar-based multi-generation system with hydrogen production. Appl Therm Eng 51:1235–1244
75. Ahmadi P, Dincer I, Rosen MA (2012) Exergo-environmental analysis of an integrated organic Rankine cycle for trigeneration. Energy Convers Manage 64:447–453
76. Ahmadi P, Dincer I, Rosen MA (2013) Development and assessment of an integrated biomass-based multi-generation energy system. Energy 56:155–166
77. Cohce M, Dincer I, Rosen M (2011) Energy and exergy analyses of a biomass-based hydrogen production system. Bioresour Technol 102:8466–8474
78. Hughes EE, Tillman DA (1998) Biomass cofiring: status and prospects 1996. Fuel Process Technol 54:127–142
79. Lian Z, Chua K, Chou S (2010) A thermoeconomic analysis of biomass energy for trigeneration. Appl Energy 87:84–95
80. Mujeebu M, Jayaraj S, Ashok S, Abdullah M, Khalil M (2009) Feasibility study of cogeneration in a plywood industry with power export to grid. Appl Energy 86:657–662
81. Tchanche BF, Lambrinos G, Frangoudakis A, Papadakis G (2011) Low-grade heat conversion into power using organic Rankine cycles—a review of various applications. Renew Sustain Energy Rev 15:3963–3979
82. Faizal M, Rafiuddin Ahmed M (2011) On the ocean heat budget and ocean thermal energy conversion. Int J Energy Res 35:1119–1144
83. Meegahapola L, Udawatta L, Witharana S (2007) The Ocean Thermal Energy Conversion strategies and analysis of current challenges. In Industrial and Information Systems, 2007 ICIIS 2007 International Conference on 123–128
84. Esteban M, Leary D (2012) Current developments and future prospects of offshore wind and ocean energy. Appl Energy 90:128–136
85. Uehara H, Nakaoka T (1984) OTEC using plate-type heat exchanger (using ammonia as working fluid). Trans Jpn Soc Mech Engineers 50:1325–1333
86. Uehara H, Ikegami Y (1990) Optimization of a closed-cycle OTEC system. J Sol Energy Eng (USA) 112(4):247–256
87. Uehara H, Miyara A, Ikegami Y, Nakaoka T (1996) Performance analysis of an OTEC plant and a desalination plant using an integrated hybrid cycle. J Sol Energy Eng 118(2):115–122
88. Yamada N, Hoshi A, Ikegami Y (2009) Performance simulation of solar-boosted ocean thermal energy conversion plant. Renew Energy 34:1752–1758
89. Cengel YA, Boles MA, Kanoğlu M (2011) Thermodynamics: an engineering approach. McGraw-Hill New York, USA
90. Bejan A, Tsatsaronis G, Moran M (1995) Thermal design and optimization. Wiley-Interscience New York, USA